U.S. DEPARTMENT OF THE INTERIOR

U.S. GEOLOGICAL SURVEY

GEOCHEMISTRY OF SURFACE SEDIMENTS IN THE GULF OF THE FARALLONES

by

Walter E. Dean[1] and James V. Gardner[2]

Open-File Report 95-527

[1]MS 939 Federal Center, Denver, CO 80225
[2]MS 999 345 Middlefield Road, Menlo Park, CA 94025

1995

TABLE OF CONTENTS

ILLUSTRATIONS

APPENDIXES

INTRODUCTION

This study was initiated to investigate the distribution, composition, and modern dispersal patterns of surface sediment on the continental shelf and slope of the Gulf of the Farallones, directly west of San Francisco, California. Results of analyses for major and trace elements, organic carbon (Corg), and calcium carbonate ($CaCO_3$) are used as fingerprints to locate sites of sediment accumulation and erosion, and to identify sediment sources in the area.

The Gulf of the Farallones (Fig. 1) is a present-day re-entrent in the otherwise relatively straight coastline of northern California. The Gulf stretches about 75 km from north to south and is less than 60 km from the shelf break to the Golden Gate. Water depths in the study area of the Gulf range from <50 m to about 120 m on the shelf and between 500 and 3000 m on the slope. The land adjacent to the Gulf consists of a relatively high, steep metamorphic terrane in the northeast and a lower sedimentary and metamorphic terrane in the southeast (Hall, 1966; California Division of Mines and Geology, 1980).

The continental shelf of the Gulf of the Farallones has a gradient of about 0.1° but the slope drops away relatively steeply at 3°. Although the shelf is uncut by channels and canyon heads, the upper slope is incised with numerous submarine canyons and gulleys, including Pioneer Canyon (Fig. 1).

The basement rocks of the Farallon region are composed of remnants of the long-lived subduction complex and accreted terranes. The oceanic crust of the Farallon Plate is represented by pillow basalts, gabbros, and diabase dikes. Pelagic sediments deposited far out in the central Pacific away from any influence of the North American Plate are represented by beds and fragments of radiolarian chert and seamount carbonate rocks. Hemipelagic and terrigenous sediments deposited over the pelagic sediments as the Farallon and North American Plates converged are represented by turbidites of graywacke, claystone, shale, and sandstone. Each of these rock types, as well as mixtures, is well exposed on the San Francisco Peninsula (Hall, 1966; Blake and others, 1984; Wahrhafig, 1984).

The drainage system through the Golden Gate was tectonically changed about 500 ka from a large, internally drained lake, and began to flow to the ocean (Hall, 1965; 1966). Since then, sediment has been deposited on the continental shelf during the numerous eustatic high stands of sea level. The Farallon shelf was subaerially exposed during major global glaciations, the most recent of which was from ~20 to ~15 ka. During these eustatic low stands, a river probably coursed across the shelf to the shelf break, although no channel has been identified to date. Since ~15 ka, the eustatic rise of sea level has allowed sediment to accumulate on the shelf. San Francisco Bay estuary receives run-off from approximately 40% of the land area of California (Conomos, 1979).

The main oceanographic influences on the western margin of the Gulf of the Farallones include the southward-flowing California Current and a counter-clockwise gyral circulation caused by the protrusion of a headland at Point Reyes (Fig. 1). The California Current is driven by northwesterly winds, primarily during the spring and summer months when the Pacific subtropical high-pressure system dominates the northeastern Pacific Ocean (Huyer and others, 1991; Strub and others, 1991). Winters are dominated by southwesterly swells punctuated by periodic Aleutian low-pressure systems that produce southwesterly winds that sweep over the region during the Winter months.

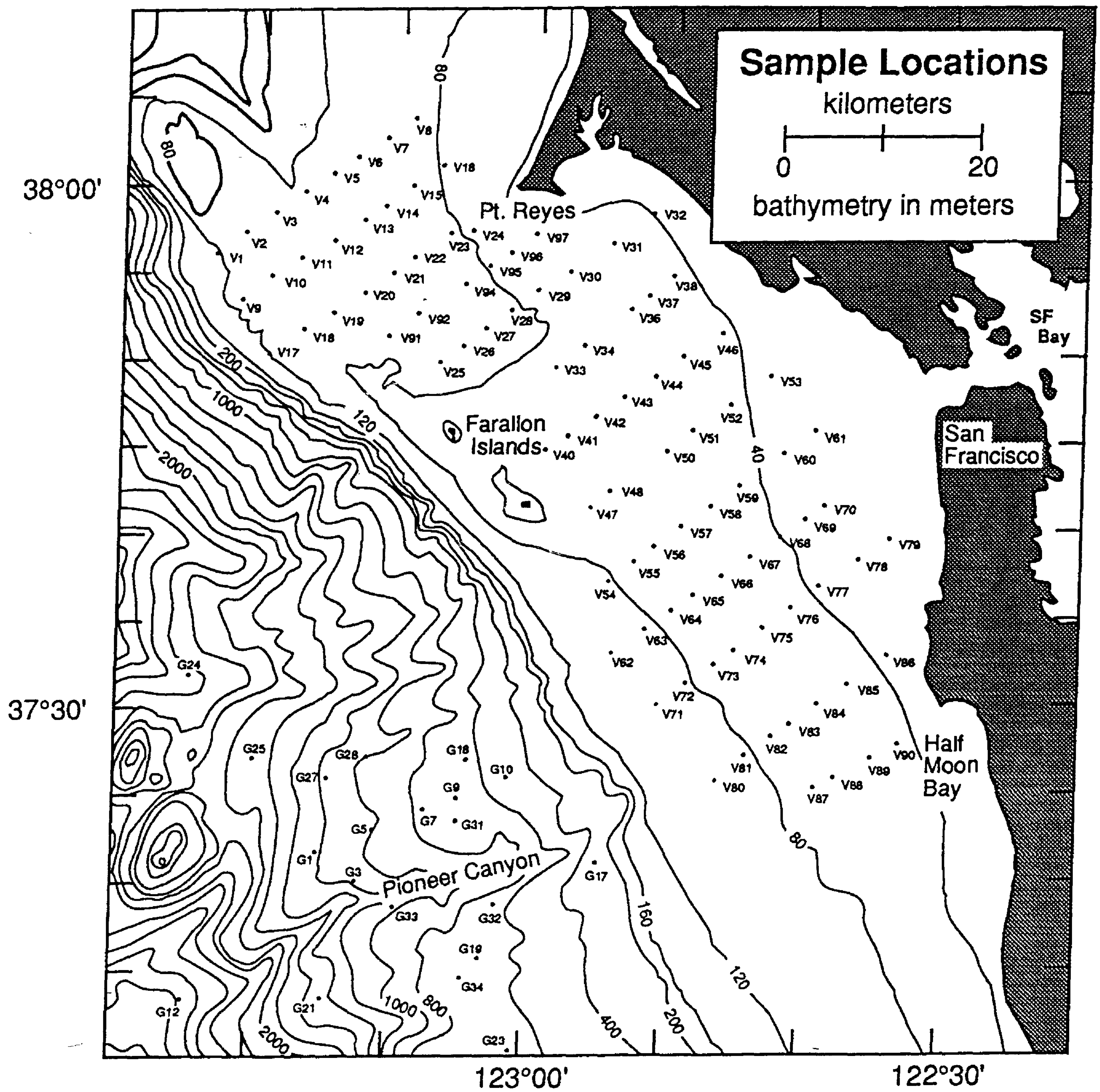

Figure 1. Index map showing locations of cores, bathymetry, and shorelines of the California continental margin from 37° N to 38°20' N, and from 122°20' W to 123°30'W.

Poleward flow, to compensate for the California Current, takes the form of northward flowing countercurrents, the Davidson Current and the California Undercurrent, with maximum velocities of up to 30 cm/sec on the upper slope in water depths of 150 to 300 m (e.g. Huyer and others, 1989; Noble and others, 1992). The countercurrent is strongest during the late fall and winter months, but appears during the summer upwelling season when northerly winds diminish (Send and others, 1987).

Coastal upwelling of cold water by Ekman transport generated by the northwesterly winds occurs as a fairly distinct "front" along most of the California margin, but "squirts", "jets", and "filaments" of cold, upwelled water commonly form off coastal promontories such as Point Reyes and extend several hundred kilometers offshore (e.g. Huyer and others, 1991; Ramp and others, 1991; Strub and others, 1991). The filaments have maximum dynamic-height ranges and velocities during the summer upwelling season (Strub and others, 1991). Strong offshore currents can be generated by these filaments (Ramp and others, 1991). Observations of an eddy between Point Reyes and Point Arena associated with a filament during two months in the summer of 1988 showed a total mass transport of sediment offshore on the order of 105 metric tons (Washburn and others, 1993). Movement of sediments across the shelf to the deep sea has important influences on primary production, but also has important implications of transport of waste in the coastal ocean (Washburn and others, 1993).

Cross-shelf currents also are generated by tides, with diurnal ranges in the Gulf of the Farallones of 6 to 9 cm/sec (Noble and Gelfenbaum, 1990; Noble and others, 1992). Tidal currents account for 35 to 60% of the total variability in the currents on the shelf in the Gulf of the Farallones, and 15 to 33% of current variability on the slope (Noble and others, 1992). Tidal currents are responsible for resuspension of sediment and transport of this sediment seaward (Noble and Gelfenbaum, 1990; Noble and others, 1992).

The oceanographic climate in the Gulf of the Farallones has two modes; a spring–summer mode and a fall–winter mode produced by the dominance of an atmospheric subtropical high pressure system and a Great Basin low during the spring and summer and an Aleutian low and Great Basin high that dominate during the fall and winter months (e.g. Huyer and others, 1991; Strub and others, 1991) The spring–summer mode is relatively storm free with coastal fog and persistent 20-kt afternoon winds. In contrast, the fall–winter mode is characterized by brief (one to two days) intense storms, followed by several days of calm conditions. Strong northwesterly or southwesterly winds from winter storms can generate large waves and swells.

METHODS

A total of 93 Soutar Van Veen cores were collected from the shelf 1989, and 19 gravity cores were collected from the slope in 1990 (Fig. 1). Surface grain-size data for all Van Veen and gravity cores are presented by Maher and others (1991) and Karl (1992), respectively.

Splits of the Van Veen and gravity core samples for geochemical analyses were air dried and ground in a ceramic mill to pass a 100 mesh sieve. Concentrations of 10 major elements (Si, Al, Fe, Mg, Ca, Na, K, Ti, P, and Mn) were measured by wavelength-dispersive X-ray fluorescence spectrometry (XRF; Baedecker, 1987). Concentrations of 27 major and trace elements (Al, Fe, Mg, Ca, Na, K, Ti, P, Mn, Ba, Ce, Co, Cr, Cu, Ga, La, Li, Nd, Ni, Pb, Sc, Sr, Th, V, Y, Yb, and Zn) were determined by inductively coupled, argon-plasma, emission spectrometry (ICP; Baedecker, 1987).

An estimate of precision of the XRF and ICP techniques were obtained by performing duplicate analyses on 9 samples of surface sediments (cores F2-89-V03, -V48, -V58, -V61, -V86, -V89, -V94, F8-90-G09, and -G32), and 8 samples from different depths in three slope cores F8-90-G21, -G25, and -G27). The percent difference between duplicates was calculated for each type of analysis (XRF and ICP) and for each group of samples (surface sediments and down core samples from G21, G25, and G27). Histograms of average and maximum percent difference between duplicates are plotted in Figure 2. Scatter plots of major-element oxide by ICP versus major-element oxide by XRF are shown in Figure 3. The histograms (Fig. 2) and the scatter plots (Fig. 3) show that although XRF has a better record of replication of major-element concentration, agreement between the two methods is quite good. The biggest difference shown by Figure 2 is the difference in precision for both XRF and ICP between the surface samples that are mostly shelf silts and sands, and the samples from slope cores G21, G25, and G27 that are mostly fine-grained muds. Most average differences in duplicate analyses for major elements by XRF in the surface-sediment duplicate group were <10%, although a few were considerably higher. By contrast, average differences in duplicate analyses for major elements by ICP in the slope-core duplicate group were <u>all</u> <1%. The only explanation that we can think of for this difference in precision between the shelf and slope sample groups is greater inhomogeneity in the shelf samples caused by coarser grain size. In other words, fine-grained, slope muds (average of 45% sand) with a more homogeneous mineralogy are more likely to yield nearly identical duplicate splits than are shelf sands (average of 74% sand) that have much more inhomogeneous mineral content. A slightly different ratio of heavy to light minerals in different splits of a shelf sand could result in completely different chemical compositions of the two splits. Although the samples were ground, they were only ground to pass a 100-mesh (0.177 mm) sieve (still sand-size range). Duplicate analyses of other sample sets that we have analyzed, consisting predominantly of fine-grained muds, usually show percent-difference histograms that look more like those for the slope-core duplicate set in Figure 2.

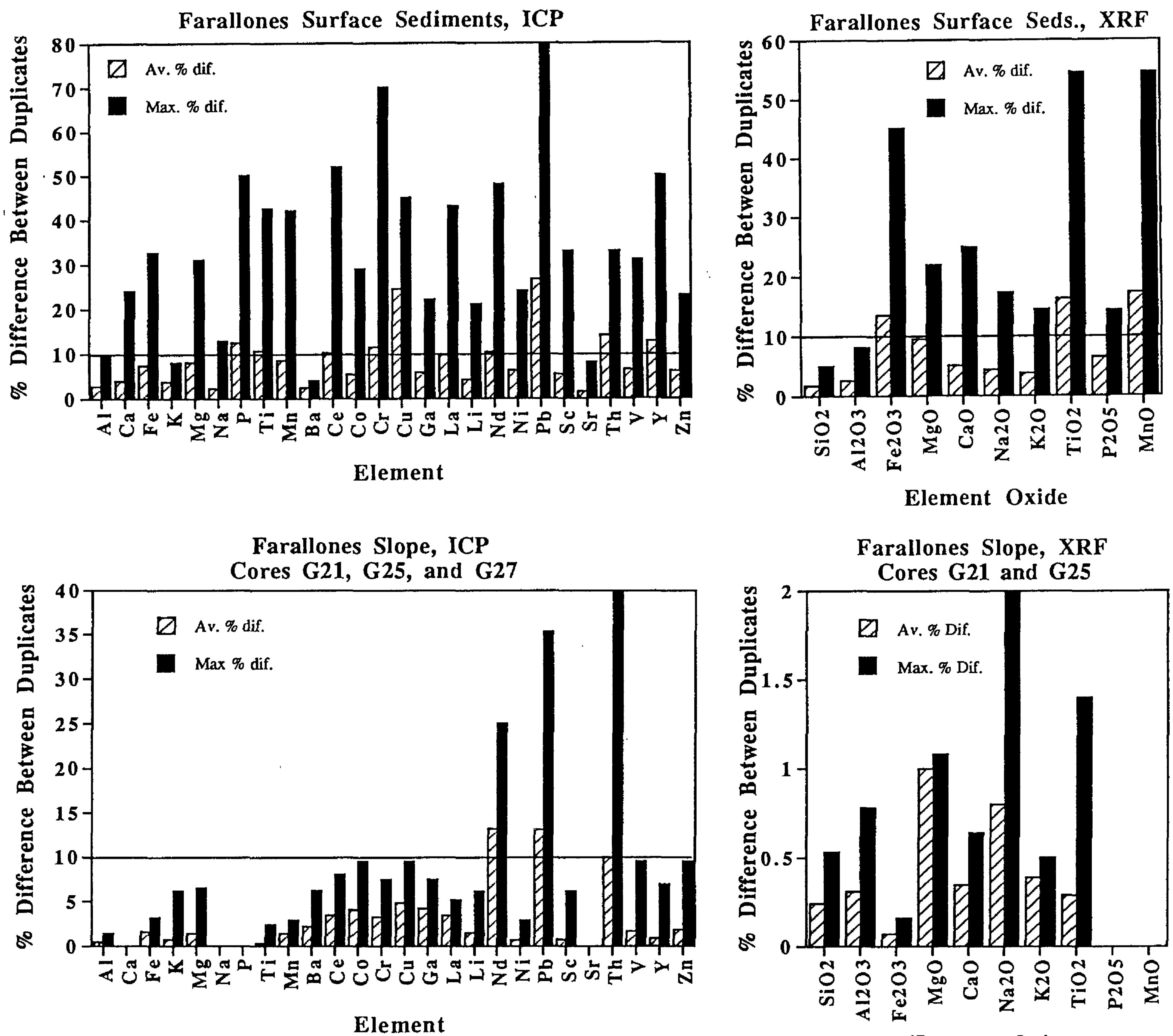

Figure 2. Histograms of maximum and average percent difference between duplicate analyses for major-element oxides and trace elements by ICP in surface sediments in shelf cores (A) and in slope cores (B), and for major element-oxides by XRF in surface sediments in shelf cores (C) and in slope cores (D).

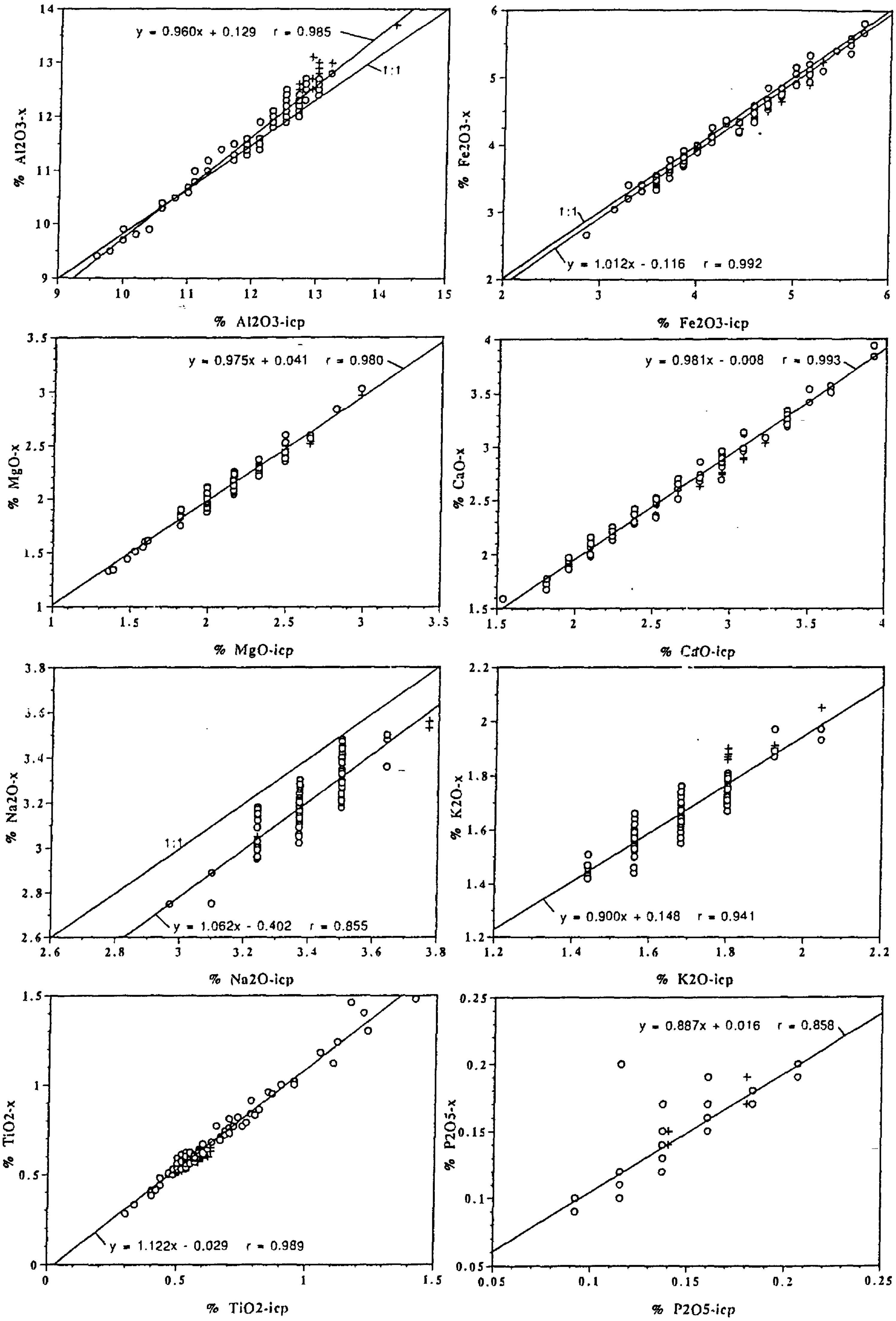

Figure 3. Scatter plots showing comparison of concentrations of major-element oxides measured by ICP and by XRF.

Concentrations of total carbon and carbonate carbon were determined by coulometry (Engleman and others, 1985) in splits of the geochemistry samples. Carbonate in the untreated sample is reacted with perchloric acid to liberate CO_2, which is then titrated in a coulometer cell to measure carbonate carbon. Total carbon is measured by liberating CO_2 by combustion of an untreated sample and titrating the CO_2. Values of organic carbon (Corg) were determined by difference between total carbon and carbonate carbon. Replicate analyses demonstrate the coulometer technique has a precision of better than ±1% for both carbonate and total carbon. Percent $CaCO_3$ was calculated by dividing percent carbonate carbon by 0.12, the fraction of carbon in $CaCO_3$.

Multivariate analysis of the geochemical data was carried out by Q-mode factor analysis to determine associations among elements, and to objectively determine geographic groupings of samples over the Gulf of the Farallones based on geochemical similarities. The computer program used is a modified version of the extended CABFAC program described by Klovan and Miesch (1976).

RESULTS

Distribution of Grain Size

Measurements of grain size for surface sediments on the Farallones margin are reported in Maher and others (1991) and Karl (1992), and a generalized map of the distribution of mean grain size based on these data (Fig. 4) is included here for of comparison with the distribution of the various geochemical parameters. Very fine sand (3-4 Φ) dominates the inner shelf and margin, whereas medium to fine sand (<3 Φ) occurs in a central area of the shelf directly offshore from the Golden Gate (Fig. 4). This distribution of coarser sediment on the shelf west of the Golden Gate may reflect relict sediment from a low-stand deposit or a winnowed lag of San Joaquin-Sacramento River sediment reworked by strong diurnal tides and major storm events. The areas of finer grain size between the Golden Gate and Half Moon Bay may represent the winnowed material that was transported in the nearshore zone away from the coarser material that lies to the northwest. Some fine-grained sediment is carried across the San Joaquin-Sacramento delta, through the Golden Gate and across the continental shelf. However, once in the mid-shelf region, the fine-grained material is intercepted by the northward-flowing undercurrent. Studies by Drake and Cacchione, 1985 and Cacchione and others (1994) show that fine-grained sediment along the mid-shelf about 100 km to the north of the Gulf of the Farallones is transported northwards offshore during strong winter storm events, and that prossibly occurs in the Gulf as well. As expected, the mean grain size decreases with increasing depth on the slope, with generaly coarser grain sizes in Pioneer Canyon (Fig. 4).

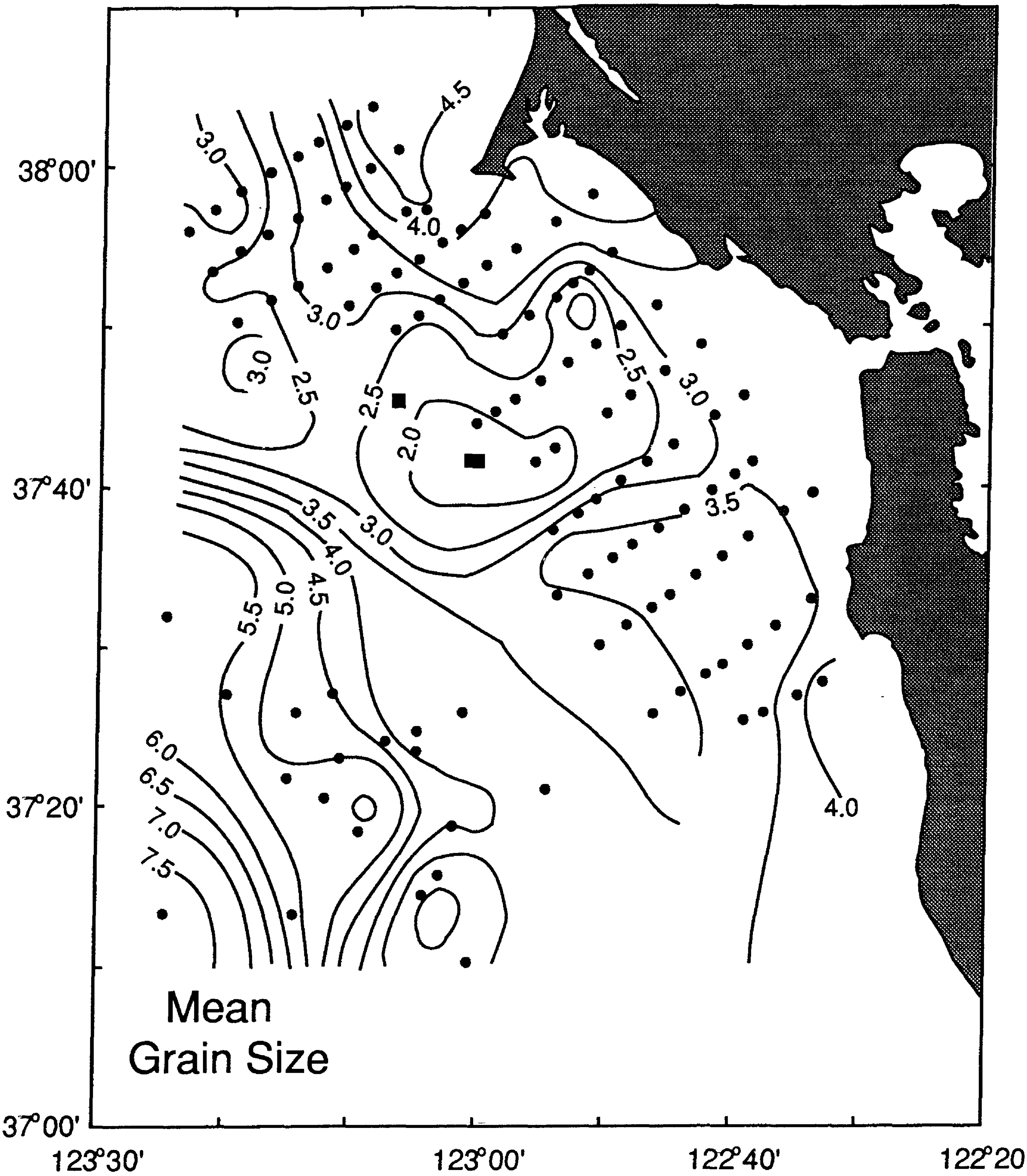

Figure 4. Map of mean grain size (in phi units, Φ) of surface sediments from the Gulf of the Farallones. Black solid squares indicate the locations of the Farallon Islands. 2-3 Φ = fine sand; 3-4 Φ = very fine sand; 4-6 Φ = coarse silt; 6-7 Φ= medium silt; 7-9 Φ= fine silt

Distribution of Element Concentrations

Results of analyses of major-element oxides, and total and inorganic carbon in samples of sediment in cores from the continental shelf and continental slope in the Gulf of the Farallones are listed in Appendixes I and II, respectively. Results of analyses of trace elements in samples of sediment in cores from the continental shelf and continental slope in the Gulf of the Farallones are listed in Appendixes II and IV, respectively.

Before running the Q-mode factor analyses, values given in the appendixes were normalized to fraction of each variable's range because of the widely differing values, ranging from fractions of a percent to thousands of parts per million. The normalized values, therefore, all ranged from 0 to 1. A number of iterative runs were made using two different similarity coefficients (correlation coefficient and cosine theta) and three different types of factor axes in multidimensional space (principal components, varimax rotation, and oblique rotation) (Klovan and Miesch, 1976; Miesch, 1981). Most runs produced two dominant factors, an iron-titanium-rare earth element (REE) factor and an organic-clay factor. Most other factors were expressing the variance in one or two elements. The best results were obtained using the correlation coefficient as a measure of similarity together with a four-factor model and varimax rotation to maximize the variance in the normalized data. Eighty-three percent of the variance in the normalized data was explained with this combination. The factor loadings represent the intensities of the composite variables. To determine which geochemical variables had the most influence in each factor, the factor loadings were correlated with the concentration of each geochemical variable. The results of this correlation analysis are given as correlation coefficients in Table 1.

Table 1. Correlation coefficients between loadings for Factors 1-4 and concentrations of major-element oxides (in wight perrcent) and trace elements (in parts per million, ppm).

Oxide or Element	Factor 1	Factor 2	Factor 3	Factor 4
SiO_2	-0.167	-0.627	-0.027	0.692
Al_2O_3	-0.214	0.626	-0.040	-0.502
Fe_2O_3	0.855	-0.049	-0.096	0.217
MgO	0.570	0.587	-0.244	-0.154
CaO	0.249	-0.102	0.576	0.470
Na_2O	-0.069	0.791	0.060	-0.372
K_2O	-0.252	0.643	0.221	-0.500
TiO_2	0.843	-0.496	-0.098	0.383
P_2O_5	0.614	0.280	0.010	-0.409
MnO	0.774	-0.527	-0.119	0.483
LOI	0.210	0.409	0.166	-0.712
Ba	0.009	0.747	-0.056	-0.190
Ce	0.845	-0.521	-0.026	0.399
Co	0.624	0.058	-0.213	0.212
Cr	0.659	-0.416	-0.081	0.268
Cu	0.428	0.782	-0.247	-0.149
Ga	-0.094	0.312	-0.263	-0.524
La	0.837	-0.540	-0.026	0.403
Li	0.299	0.841	-0.229	-0.561
Nd	0.860	-0.473	-0.019	0.362
Ni	0.462	0.781	-0.339	-0.361
Pb	0.109	-0.102	0.068	-0.076
Sc	0.680	-0.100	-0.187	0.100
Sr	-0.281	0.023	0.671	0.268
Th	0.749	-0.341	-0.003	0.321
V	0.840	-0.120	-0.217	0.244
Y	0.825	-0.410	-0.117	0.216
Yb	0.788	-0.274	-0.093	0.154
Zn	0.583	0.744	-0.269	-0.256
Corg	0.292	0.830	-0.223	-0.451
$CaCO_3$	0.035	0.127	0.807	0.362

Factor 1 explained 38% of the variance in the normalized data. Table 1 shows that Factor 1 loadings have high correlation coefficients ($r>5.0$) with many geochemical variables. Those variables (elements or oxides) that have the most influence on Factor 1, in order of decreasing importance (decreasing value of correlation coefficient; Table 1), are: La, Fe_2O_3, Nd, TiO_2, Ce, V, Y, Yb, MnO, Th, Sc, Cr, Co, P_2O_5, Zn, and MgO. Contour maps of Factor 1 loadings and concentrations of most of the Factor 1 elements over the Farallones margin are shown in Figure 5.

Sediments with highest loadings for Factor 1 (Fig. 5A), as typified by concentrations of Fe_2O_3 >5.0% and TiO_2 >1.4% (Figs. 5B and D), have maximum concentrations of Factor 1 elements in an area between the Golden Gate and the Farallon Islands. Some of the Factor 1 elements (La, Ce, MnO, Th, and Cr) show a minor concentration of Factor 1 centered on the

Farallon Islands, whereas other Factor 1 elements (Fe_2O_3, TiO_2, P_2O_5, and MgO) have low concentrations in sediments around the Farallon Islands. This distribution of Factor 1 sediments falls within the sand-rich belt around the Farallon Islands (Fig. 4) and probably reflects deposits of heavy-mineral components in relict sediment that has been continuously reworked by the fluctuations of eustatic sea level and major (100-yr) storms. The heavy minerals probably were derived from the metamorphic rocks of the Franciscan Complex that the San Joaquin–Sacramento River system traverses as it approaches the bay. The bullseye of relatively low values of Fe_2O_3, TiO_2, P_2O_5, and MgO (Figs. 5C, D, L, and M) around the Farallon Islands probably reflects the composition of sand derived from the granitic islands.

Factor 2 explained 25.5% of the variance in the normalized data. Table 1 shows that Factor 2 is essentially a clay-Corg factor. Those variables (elements or oxides) that had the most influence on Factor 2, in order of decreasing importance (decreasing value of correlation coefficient; Table 1), are: Li, Corg, Na, Cu, Ni, Zn, Ba, K, Al_2O_3, and MgO. Contour maps of Factor 2 loadings and concentrations of most of the Factor 2 elements over the Farallones margin are shown in Figure 6.

The distribution of sediments with high loadings for Factor 2 (Fig. 6A) reflects the downslope decrease in grain size (Fig. 4) and concomitant increase in Corg content (Fig. 6B). The higher clay content of Factor 2 sediments is expressed in the higher concentrations of Li, Na, K, Al_2O_3, and MgO. The higher concentrations of Cu, Ni, and Zn in Factor 2 sediments are related to enrichment of these metals in Corg-rich sediments (Vine and Tourtelot, 1970; Brumsack, 1986; Holland, 1989). The relations between %Corg and concentrations of these three metals are shown in Figure 7, and are clearly better developed in the finer grained slope sediments. The concentrations of Corg (Fig. 6B) are relatively high for a continental shelf and margin, reflecting the high productivity supported by the nutrient-rich seasonal upwelling. Higher concentrations of Ba associated with siliceous biogenic debris (e.g. Dymond, 1992) probably accounts for the higher concentrations of Ba in Corg-rich Factor 2 sediments (Fig. 6H). Concentrations of Corg, Ba, and several trace metals (esp. Cr, Cu, Ni, V, and Zn) in sediment-trap samples increased markedly following a spring diatom bloom off shore from the Russian River in northern California (Dean and Gardner, unpublished data). Notice that the distribution of MgO (Fig. 5M) has high concentrations in shelf sands (Factor 1 sediments) reflecting mafic heavy minerals, and slope muds reflecting a clay-mineral association. The concentration of P_2O_5 correlates most highly with Factor 1 loadings (Table 1) but does increase downslope (Fig. 5L) reflecting an association with organic carbon.

Calcium carbonate is a very minor constituent of surface sediments, with values mostly less than 1% over the entire margin (Fig. 8A). The distribution of $CaCO_3$ is dominated by a bullseye on the northern portion of the Gulf of the Farallones probably caused by occasional bivalve fragments. Factor 3 loadings reflect this distribution of $CaCO_3$ (Table 1). Although the concentration of Sr also is correlated with Factor 3 loadings (Table 1), the distribution of Sr in surface sediments (Fig. 7B) is very different from that of $CaCO_3$ suggesting that most of the Sr is contributed from detrital clastic material rather than from the very little $CaCO_3$ that is present.

Table 1 shows that most of the contribution to Factor 4 loadings is from SiO_2, Minor contributions to Factor 4 loadings come from CaO, TiO_2, MnO, Ce, La, and Nd, but the variance in these oxides and elements is mainly accounted for by Factor 1 or, for CaO, by Factor 3. A map showing the concentration of SiO_2 over the Farallones margin is shown in Figure 9.

Concentrations of SiO_2 are generally 67% to 69% on the shelf with distinctly higher values (>70% up to 77%) adjacent to the Farallon Islands reflecting granitic sand shed from the islands (Fig. 4). Values of SiO_2 also tend to decrease downslope reflecting the downslope increase in clay. The higher concentrations of SiO_2 on the slope at the southern end of the study area probably reflects larger amounts of sand moving down Pioneer Canyon (Fig. 1). The contrast in composition between quartz-rich granitic sands and heavy-mineral-rich sands is clearly shown in Figure 10 by the negative correlation between SiO_2 and Al_2O_3, Fe_2O_3, and MgO in shelf sands. Concentrations of Al_2O_3, Fe_2O_3, and MgO in the fine-grained slope muds are fairly constant.

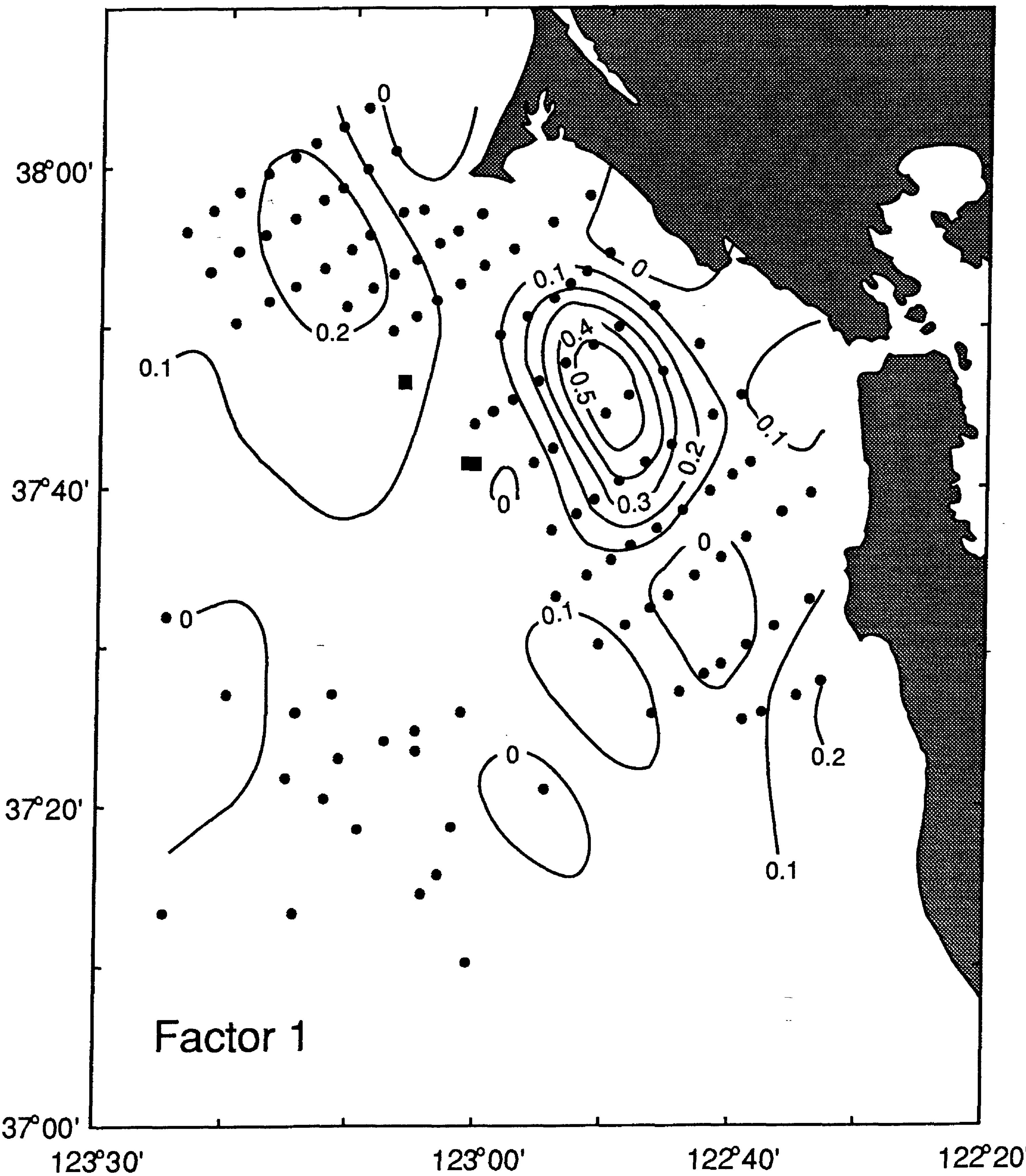

Figure 5. Maps of Factor 1 loadings (A), ppm La (B), $\%Fe_2O_3$ (C), $\%TiO_2$ (D), ppm Ce (E), ppm V (F), %MnO (G), ppm Th (H), ppm Sc (I), ppm Cr (J), ppm Co (K), $\%P_2O_5$ (L), and %MgO (M) in surface sediments from the Gulf of the Farallones. Black solid rectangles indicate the locations of the Farallon Islands.

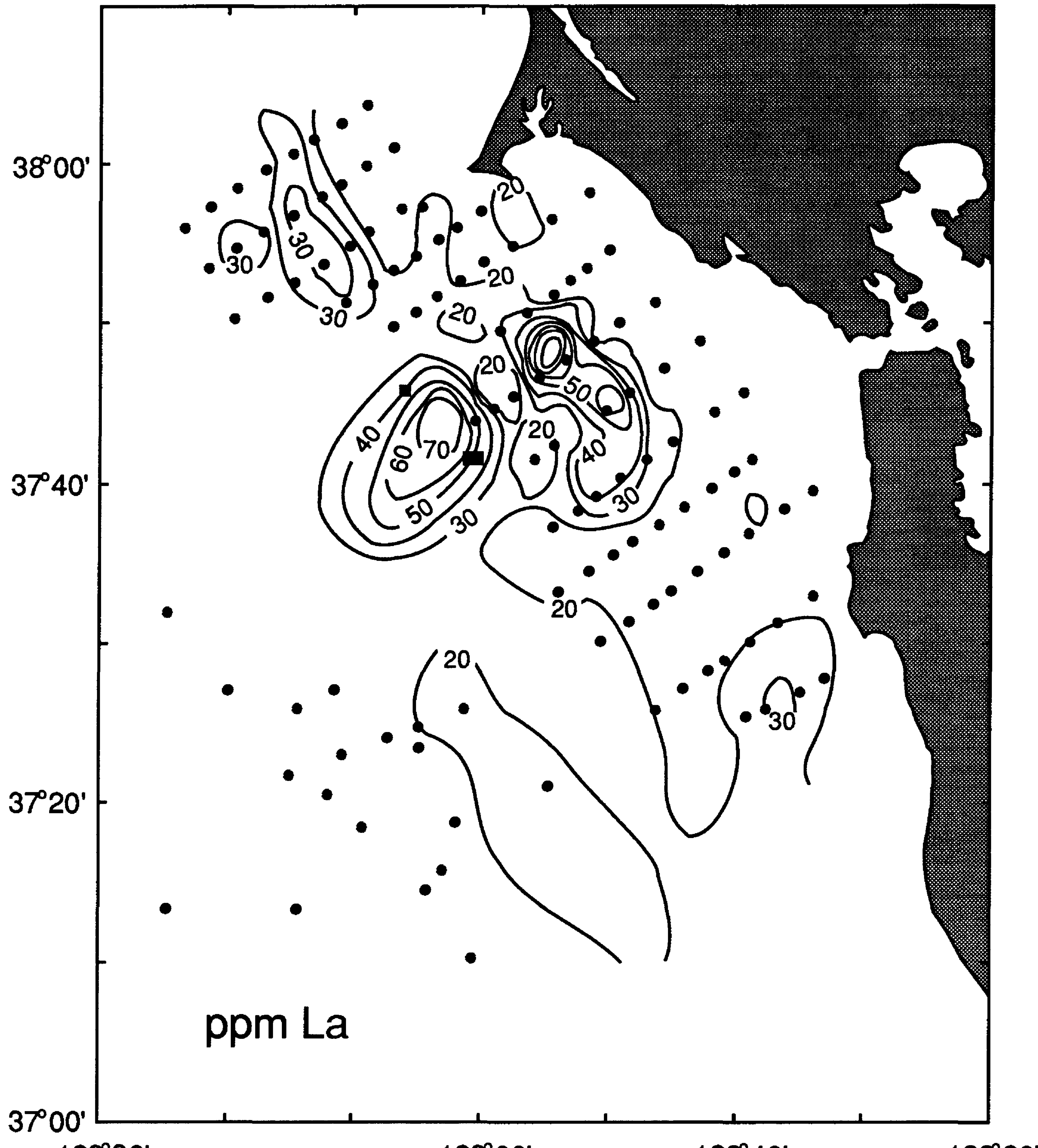

Figure 5B. Map of ppm La in surface sediments.

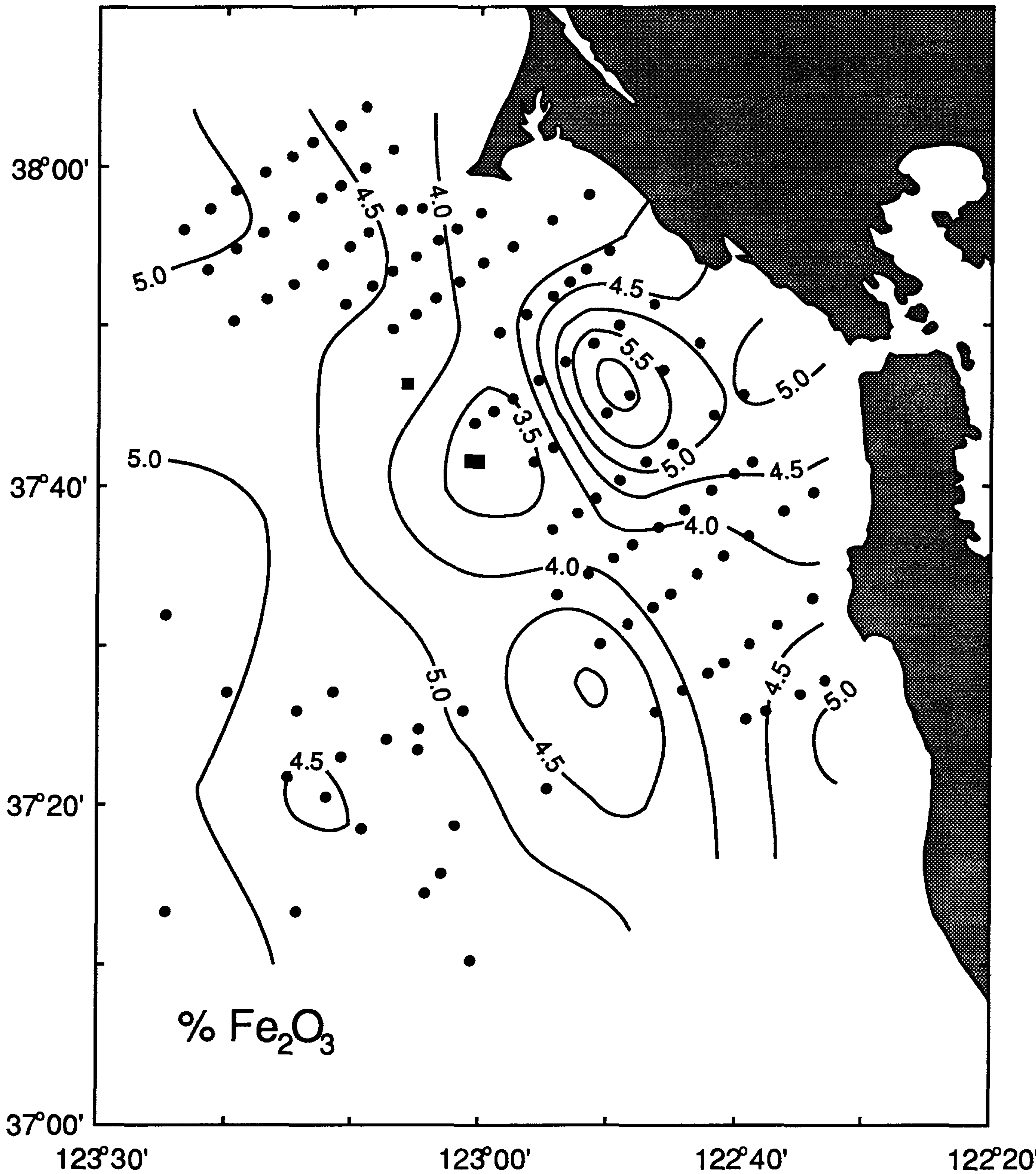

Figure 5C. Map of % Fe2O3 in surface sediments.

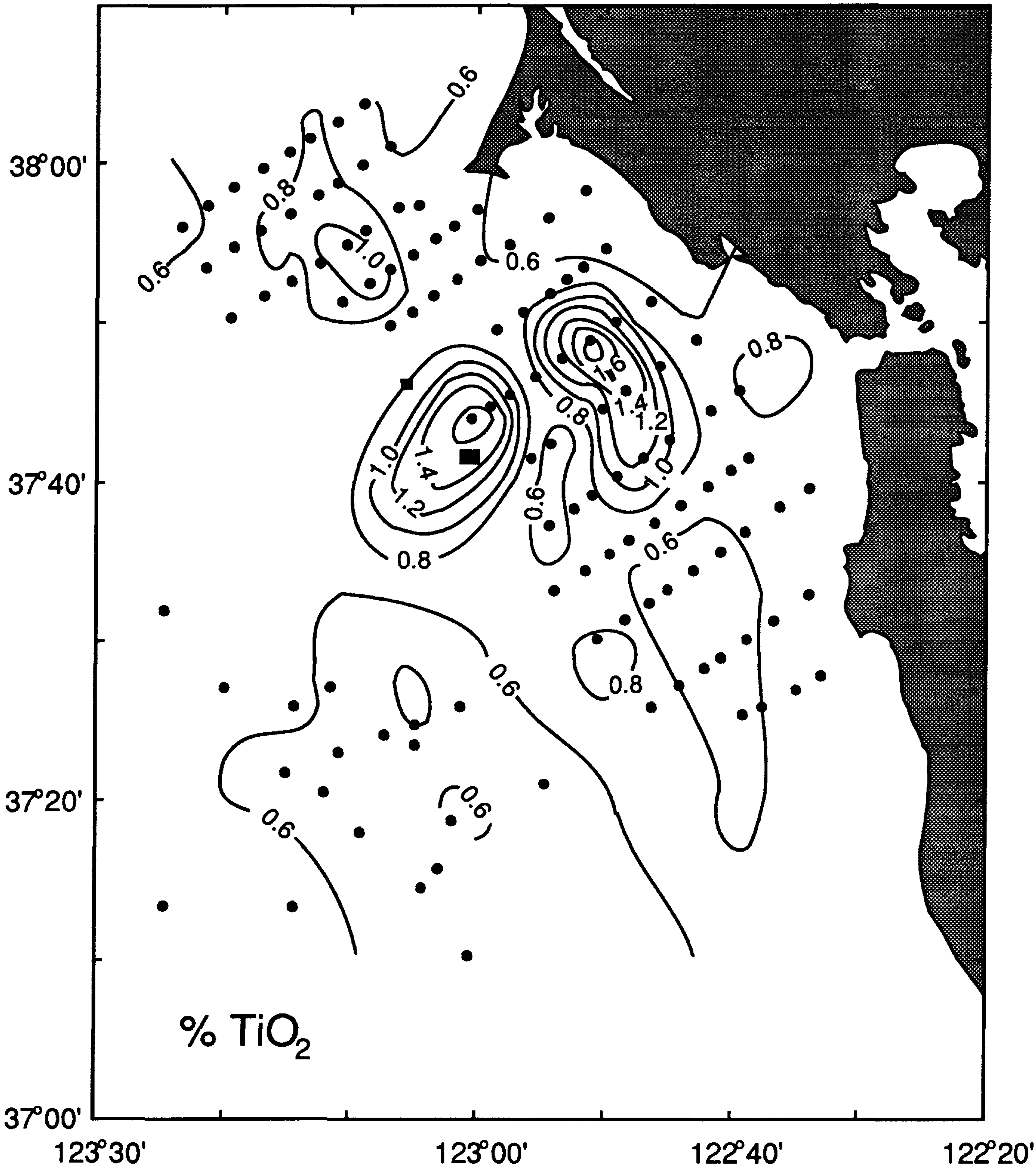

Figure 5D. Map of % TiO2 in surface sediments.

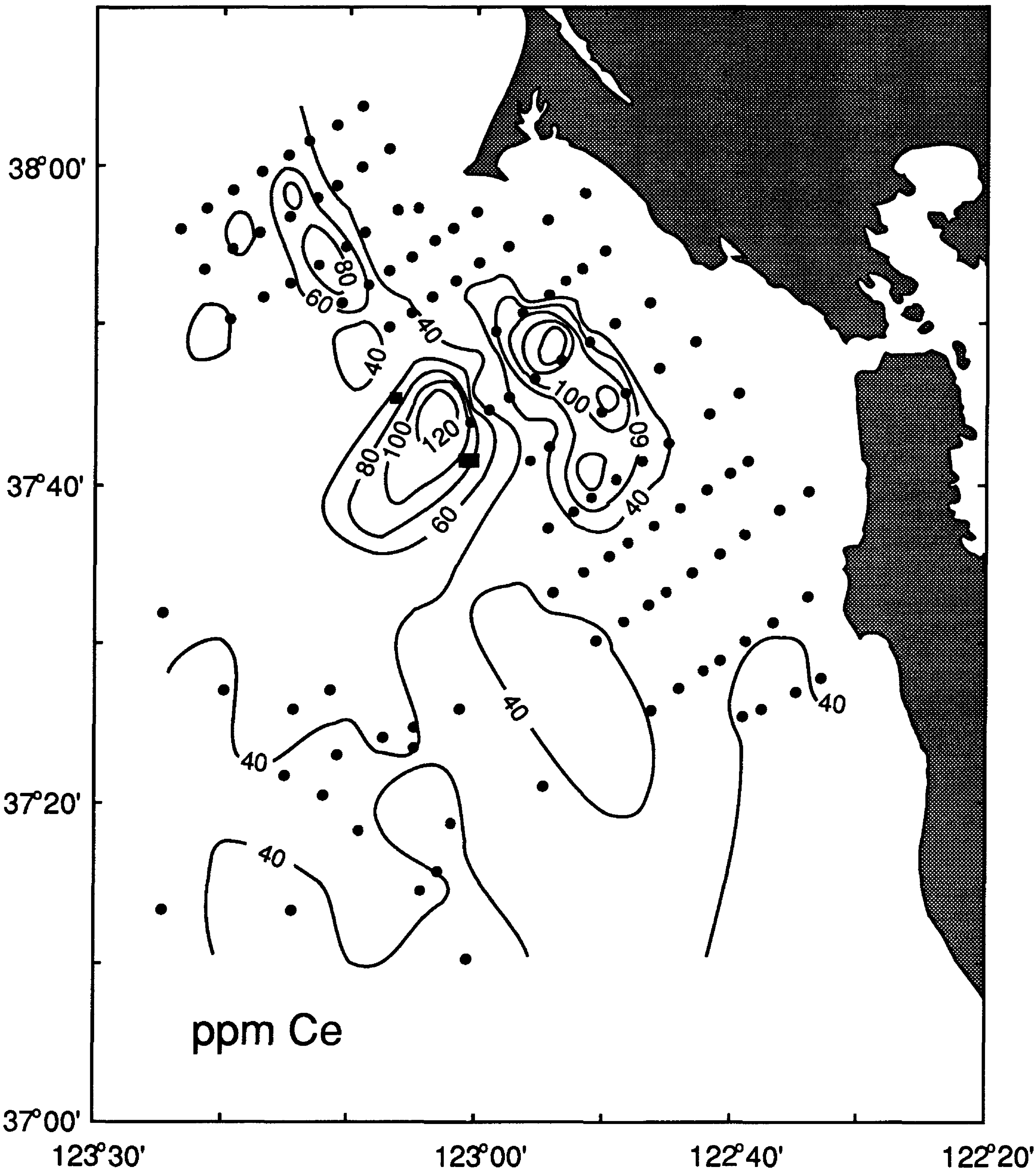

Figure 5E. Map of ppm Ce in surface sediments.

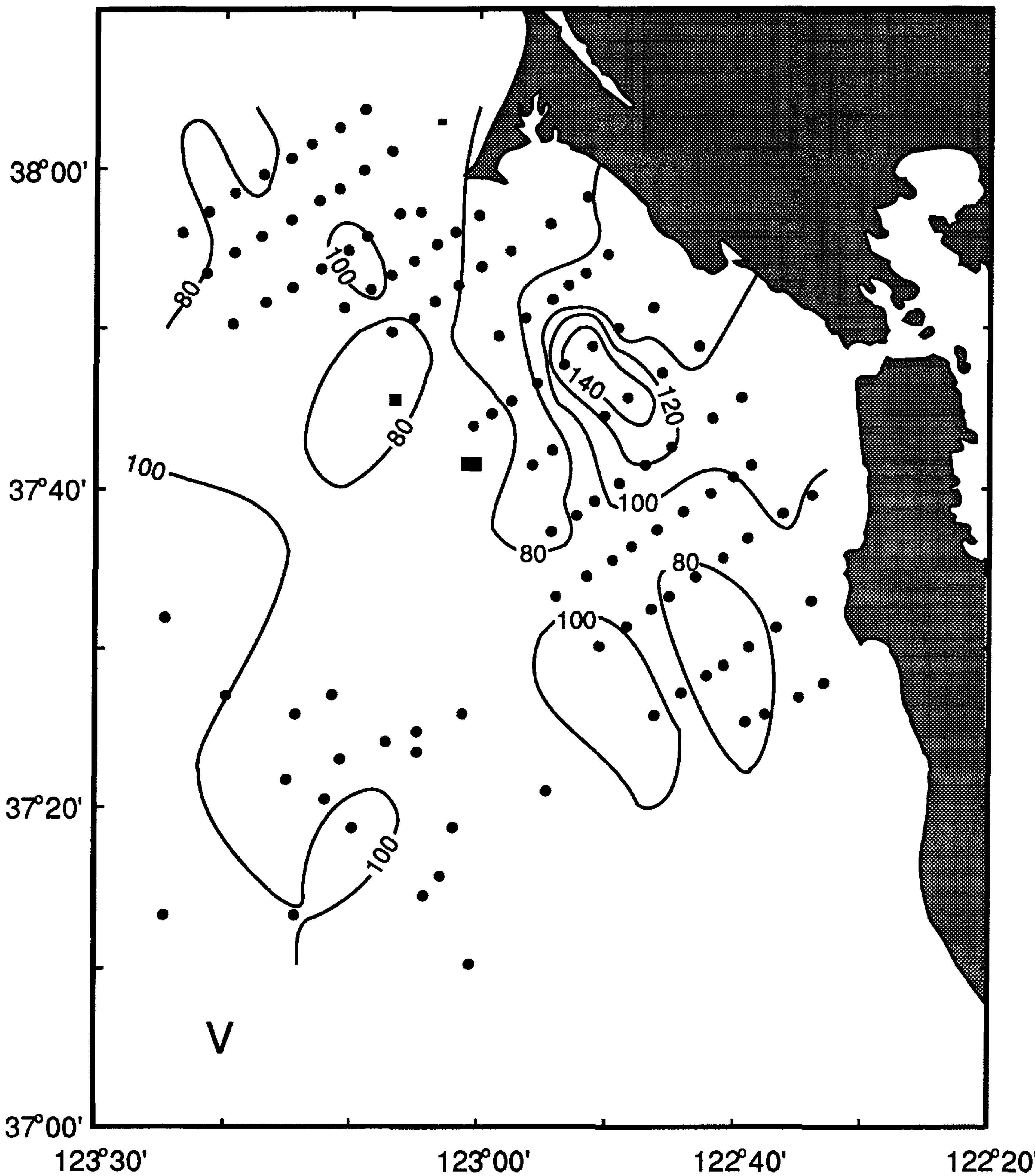

Figure 5F. Map of ppm V in surface sediments.

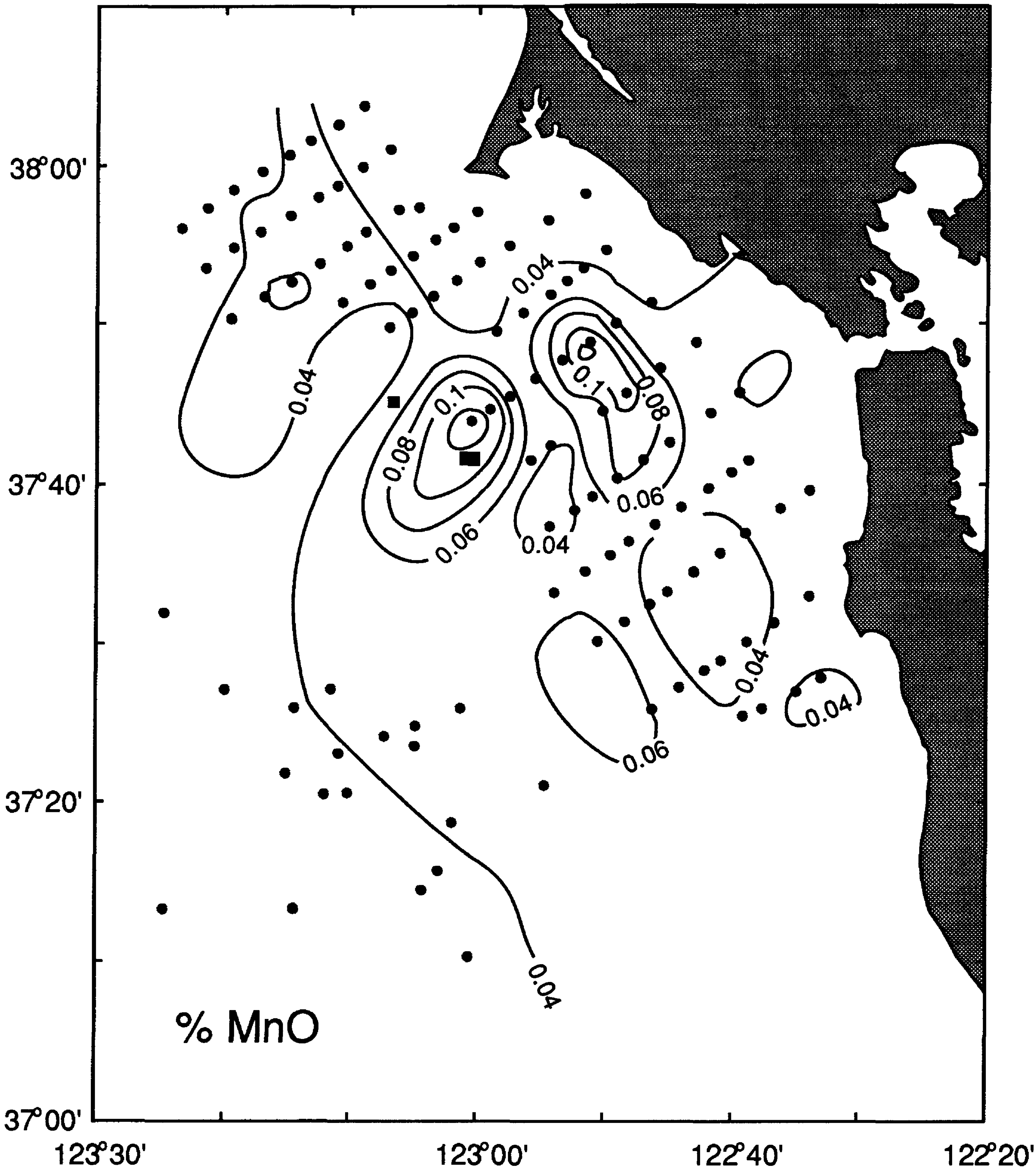

Figure 5G. Map of % MnO in surface sediments.

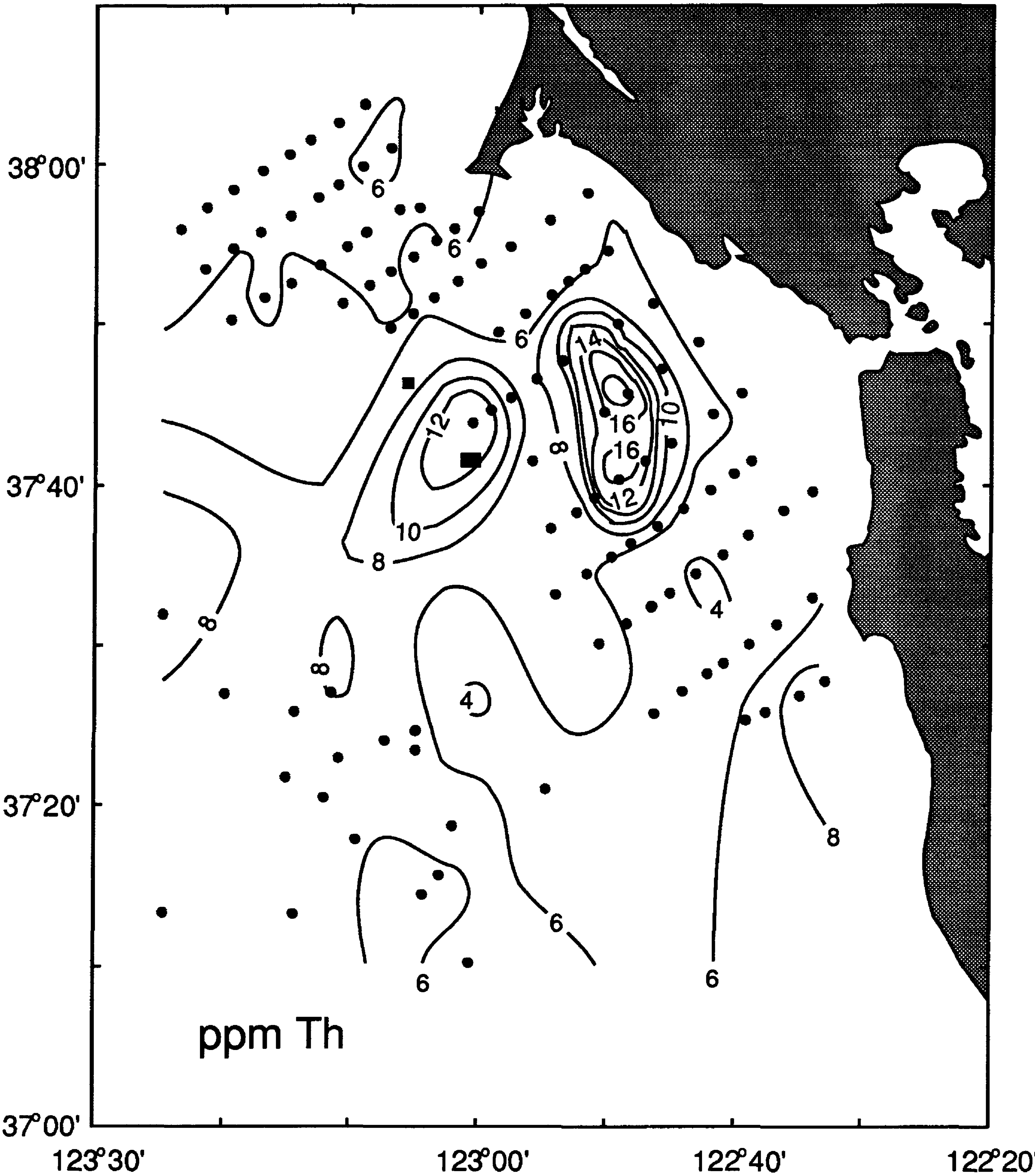

Figure 5H. Map of ppm Th in surface sediments.

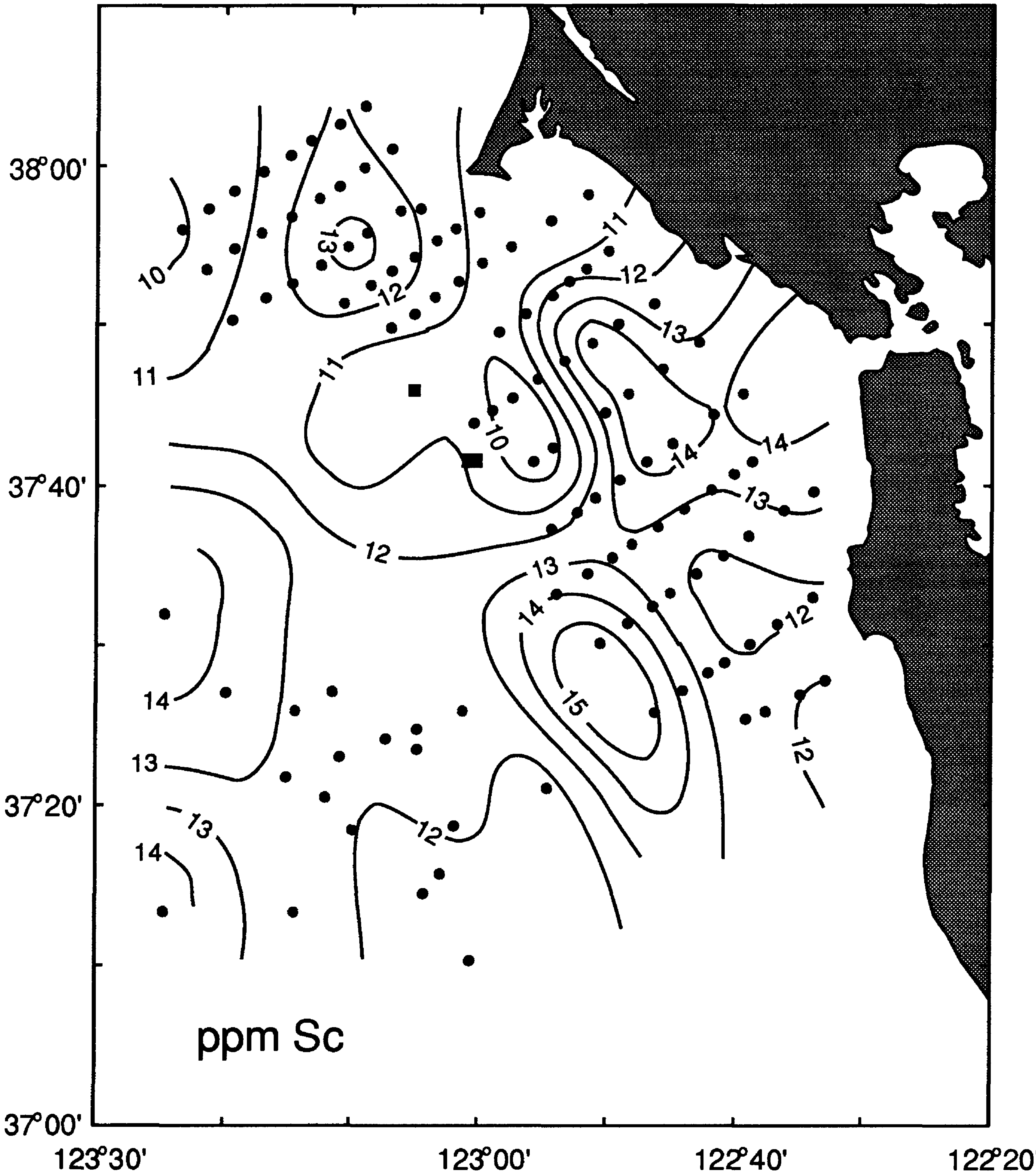

Figure 5l. Map of ppm Sc in surface sediments.

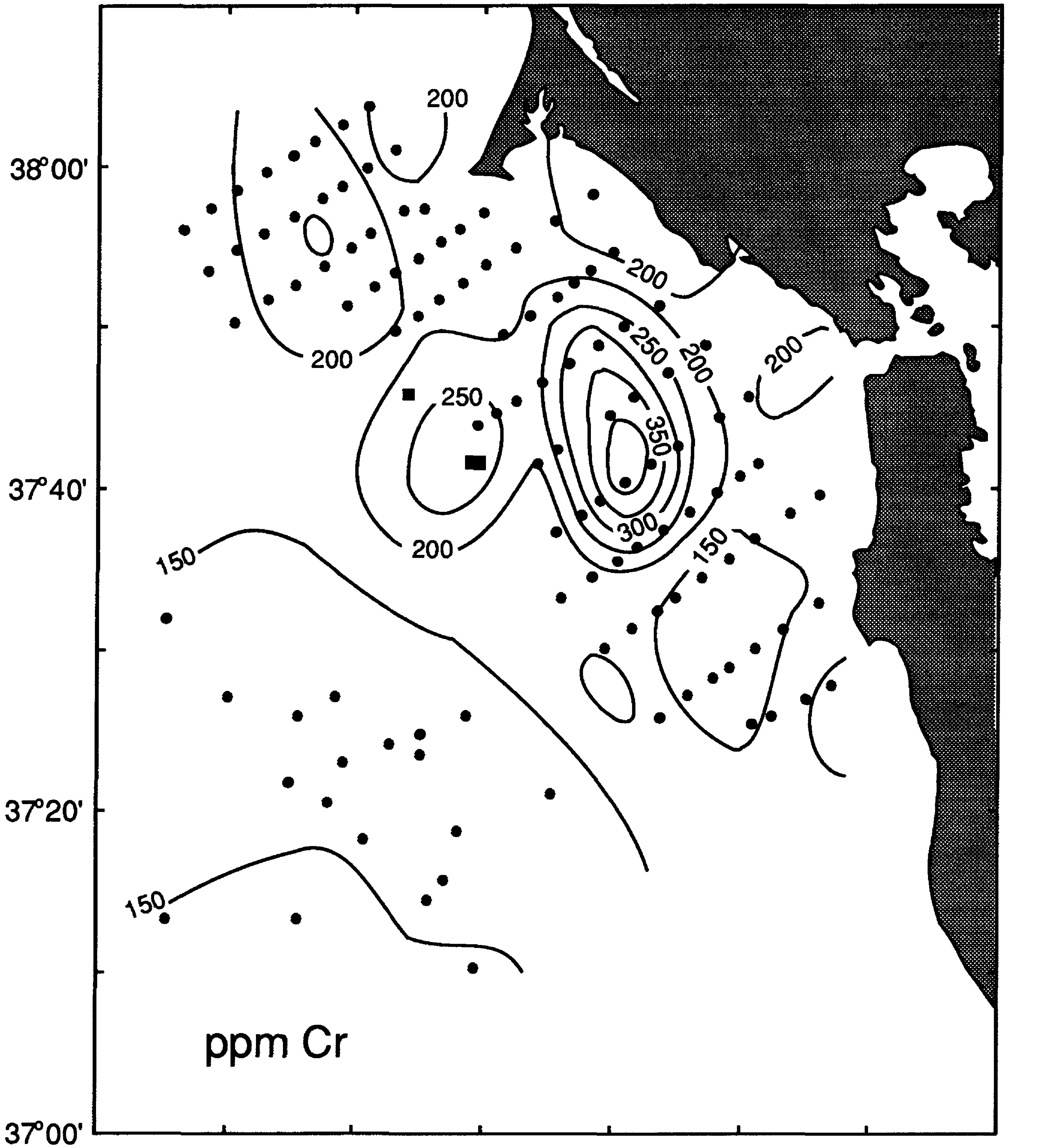

Figure 5J. Map of ppm Cr in surface sediments.

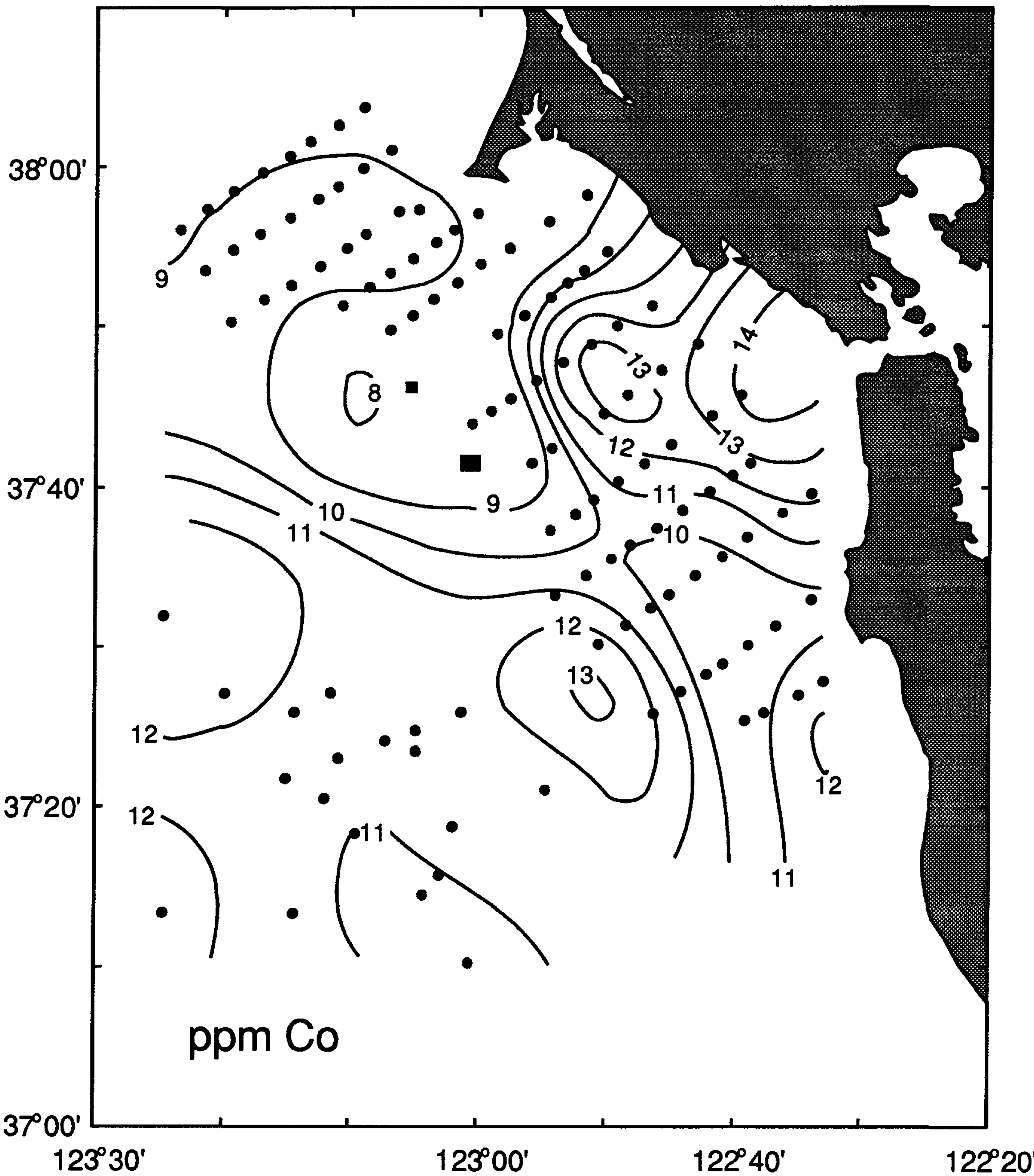

Figure 5K. Map of ppm Co in surface sediments.

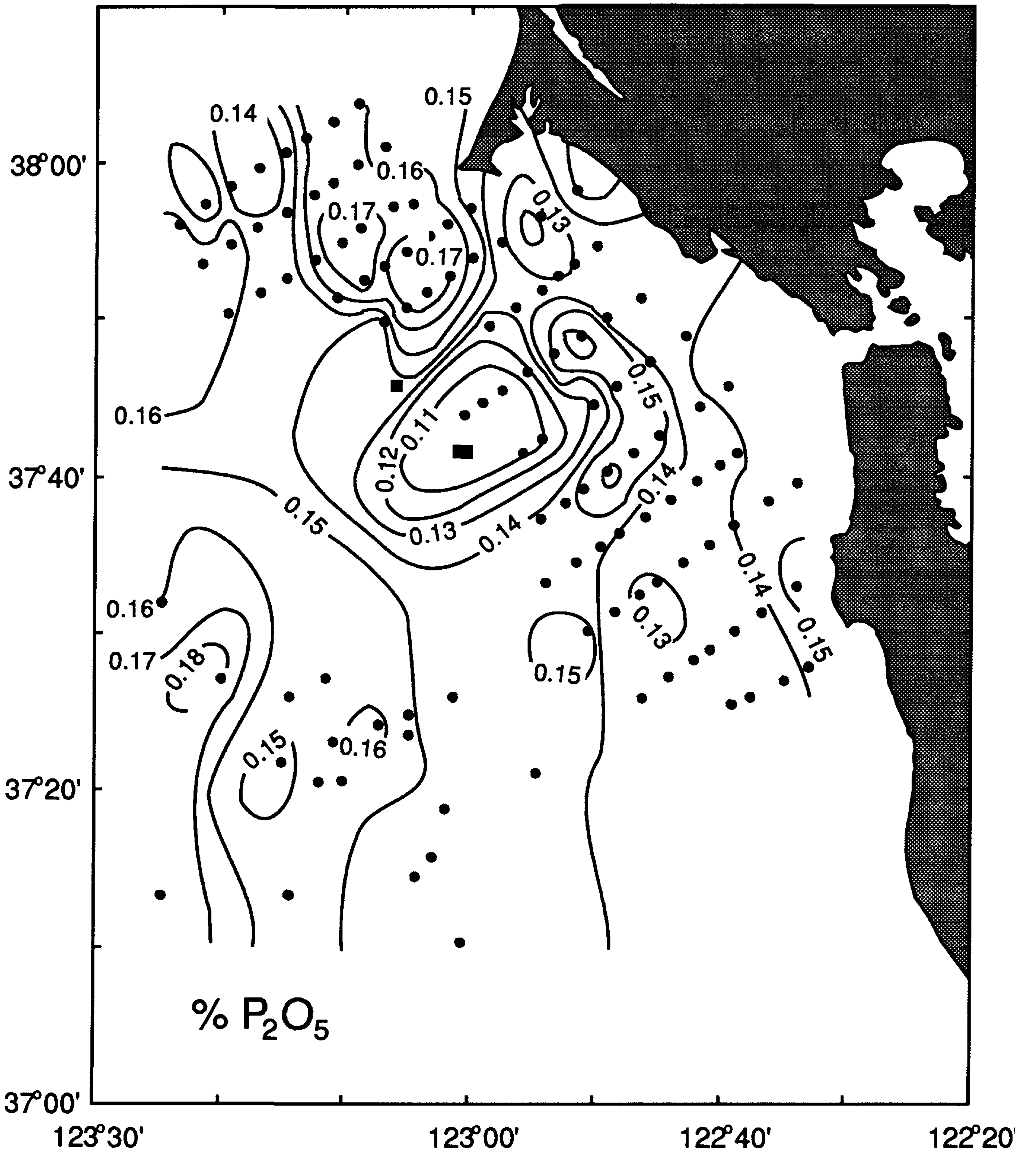

Figure 5L. Map of % P2O5 in surface sediments.

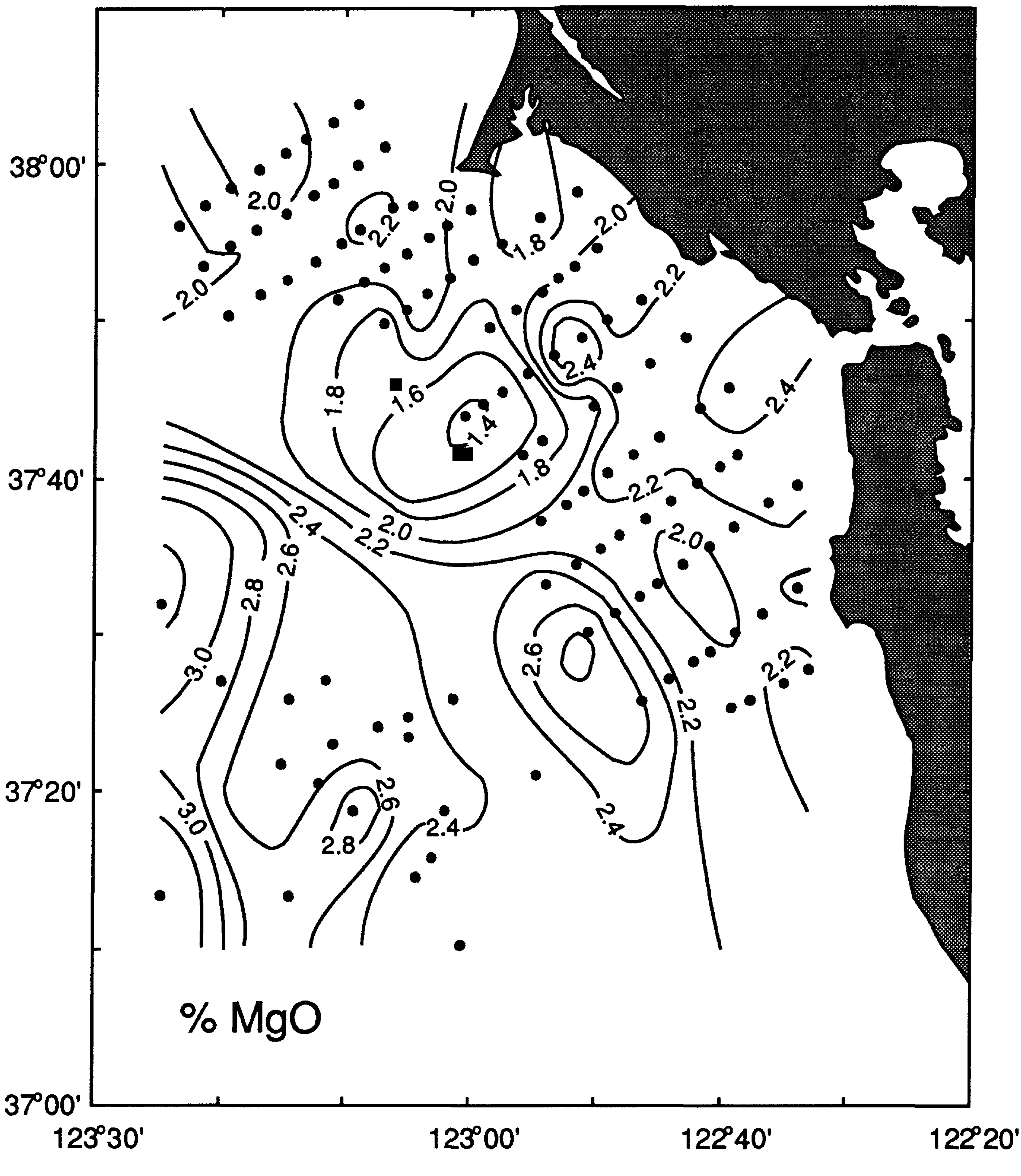

Figure 5K. Map of % MgO in surface sediments.

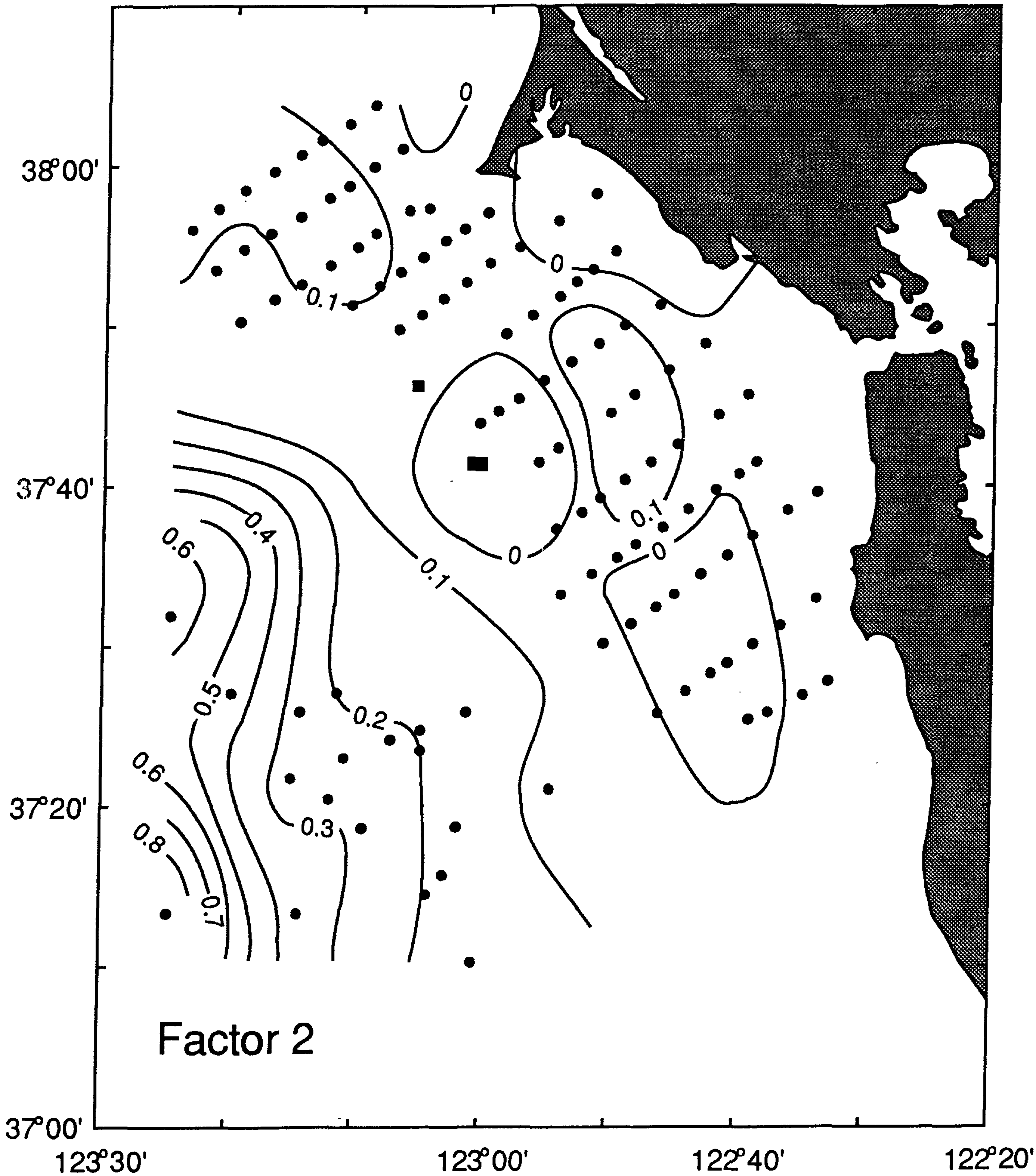

Figure 6. Maps of Factor 2 loadings (A), %Corg (B), ppm Li (C), $\%Na_2O$ (D), ppm Cu (E), ppm Ni (F), ppm Zn (G), ppm Ba (H), $\%K_2O$ (I), and $\%Al_2O_3$ (J) in surface sediments from the Gulf of the Farallones. Black solid rectangles indicate the locations of the Farallon Islands.

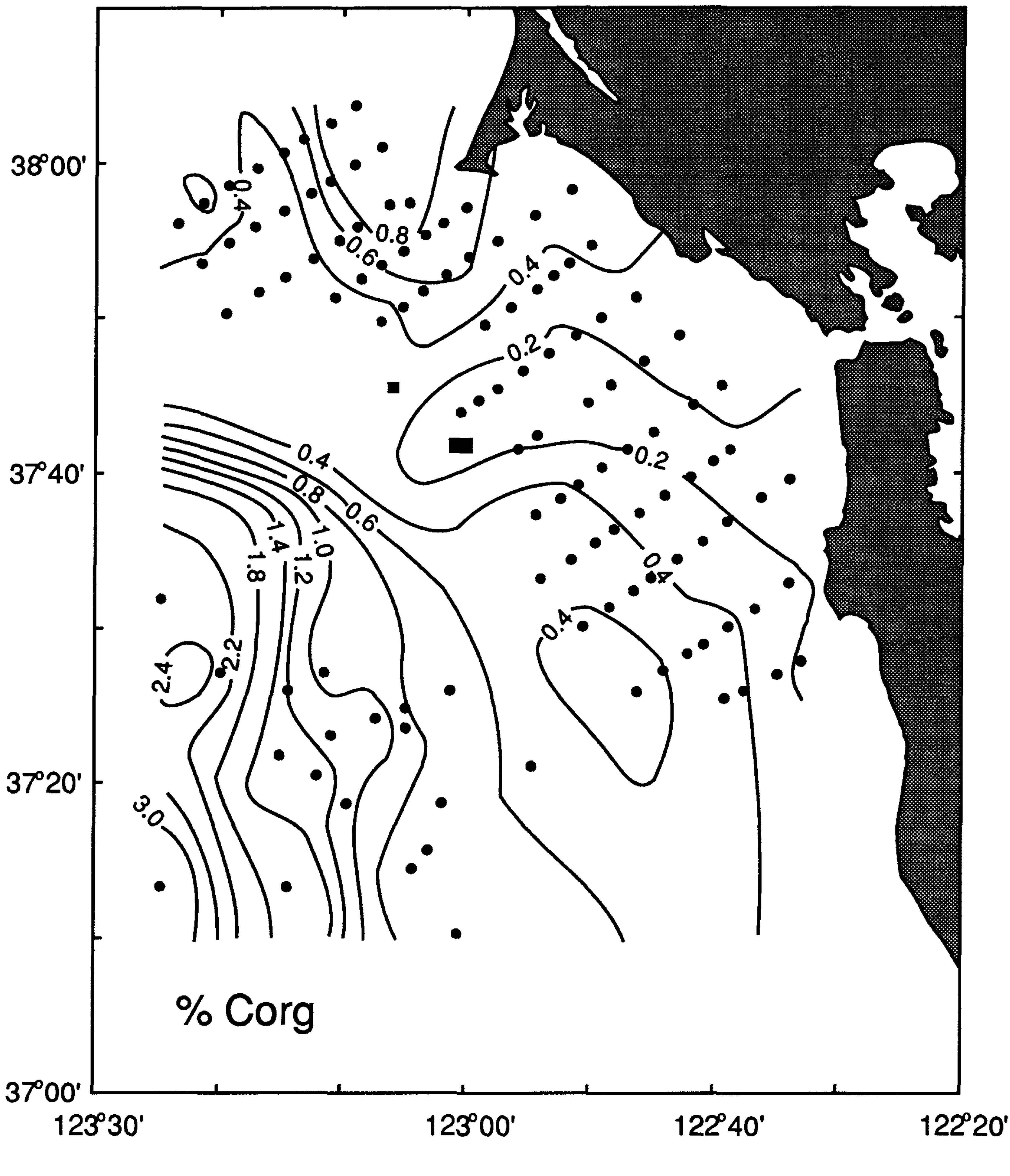

Figure 6B. Map of % organic carbon (Corg) in surface sediments.

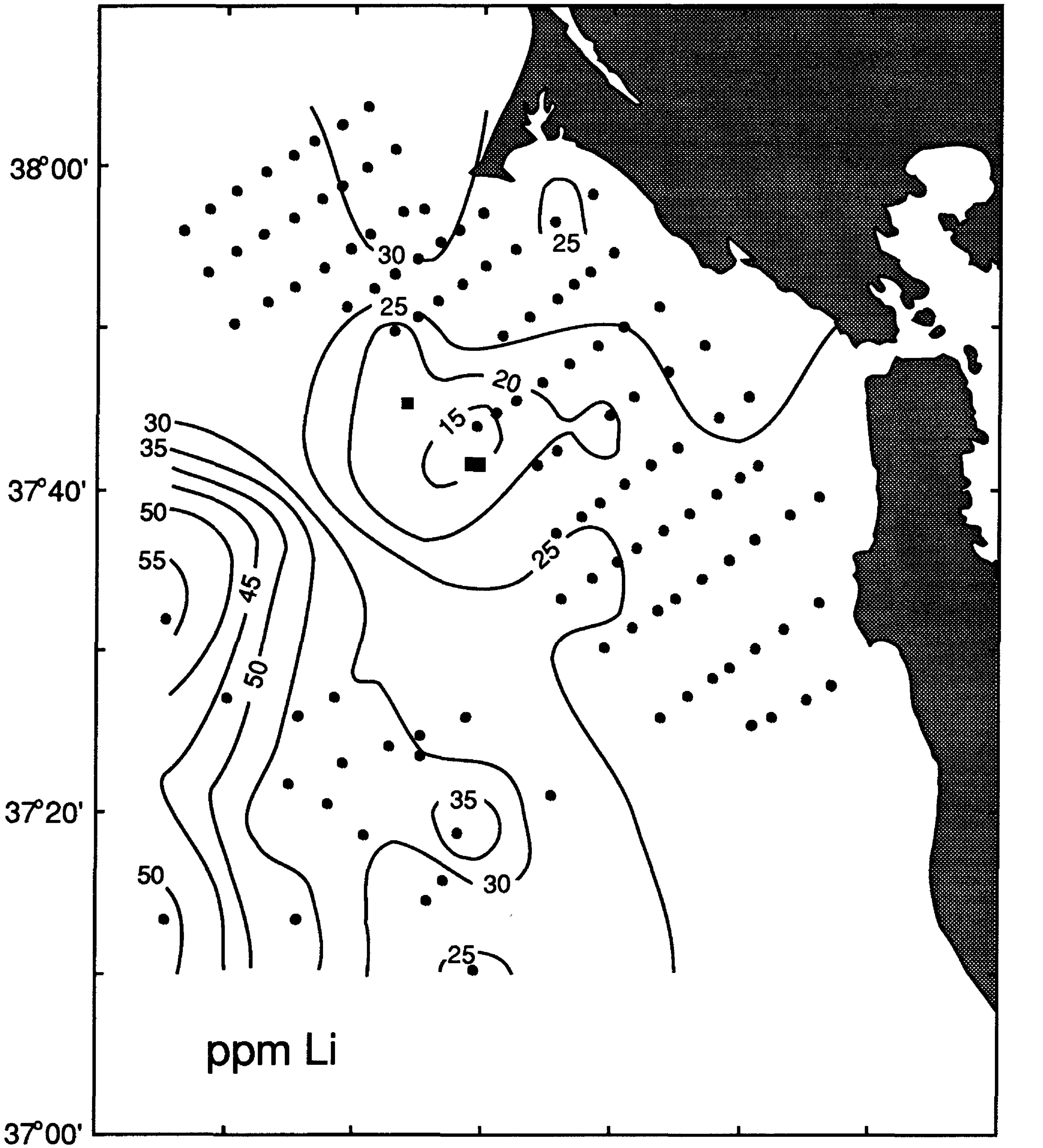

Figure 6C. Map of ppm Li in surface sediments.

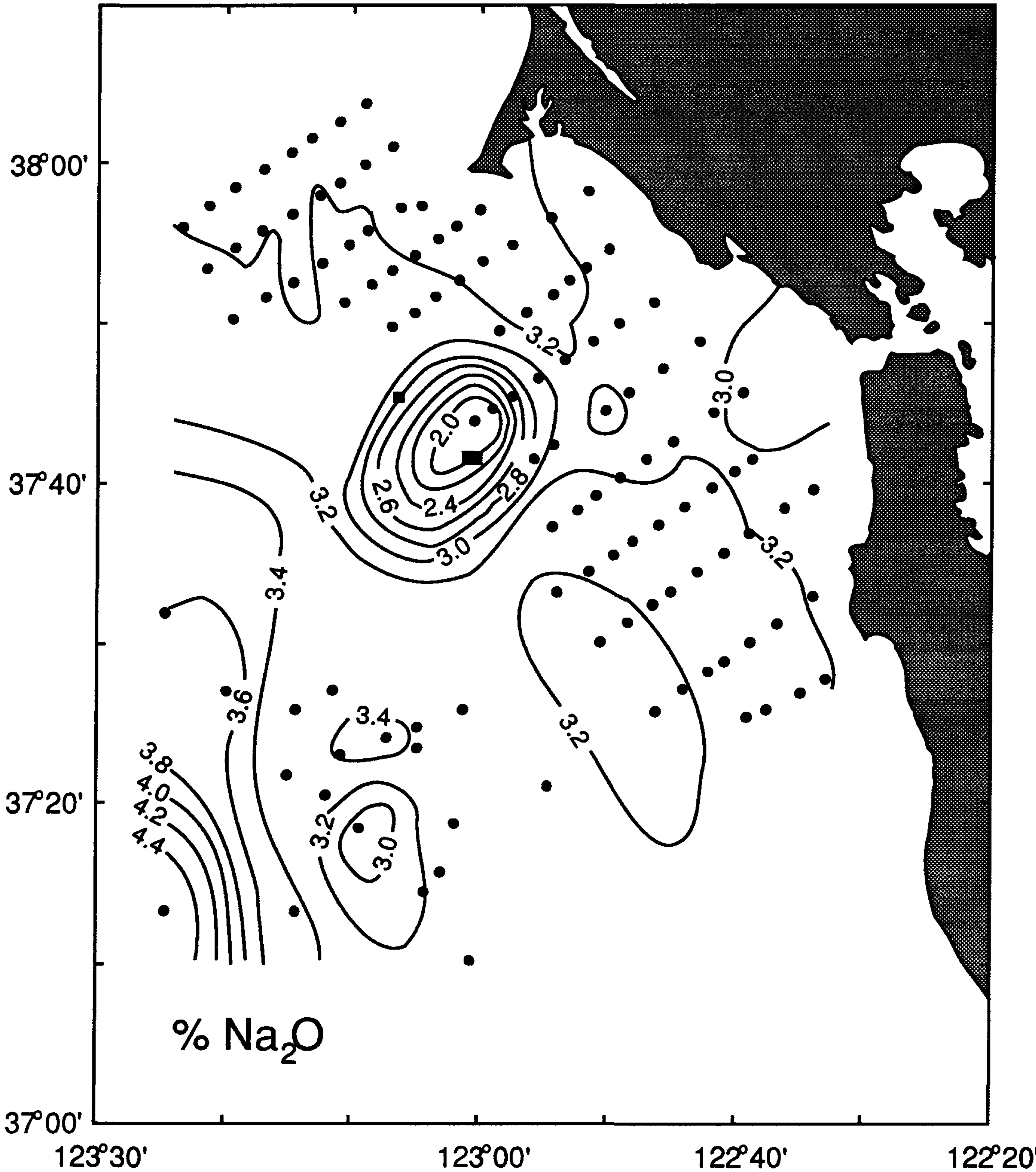

Figure 6D. Map of % Na2O in surface sediments.

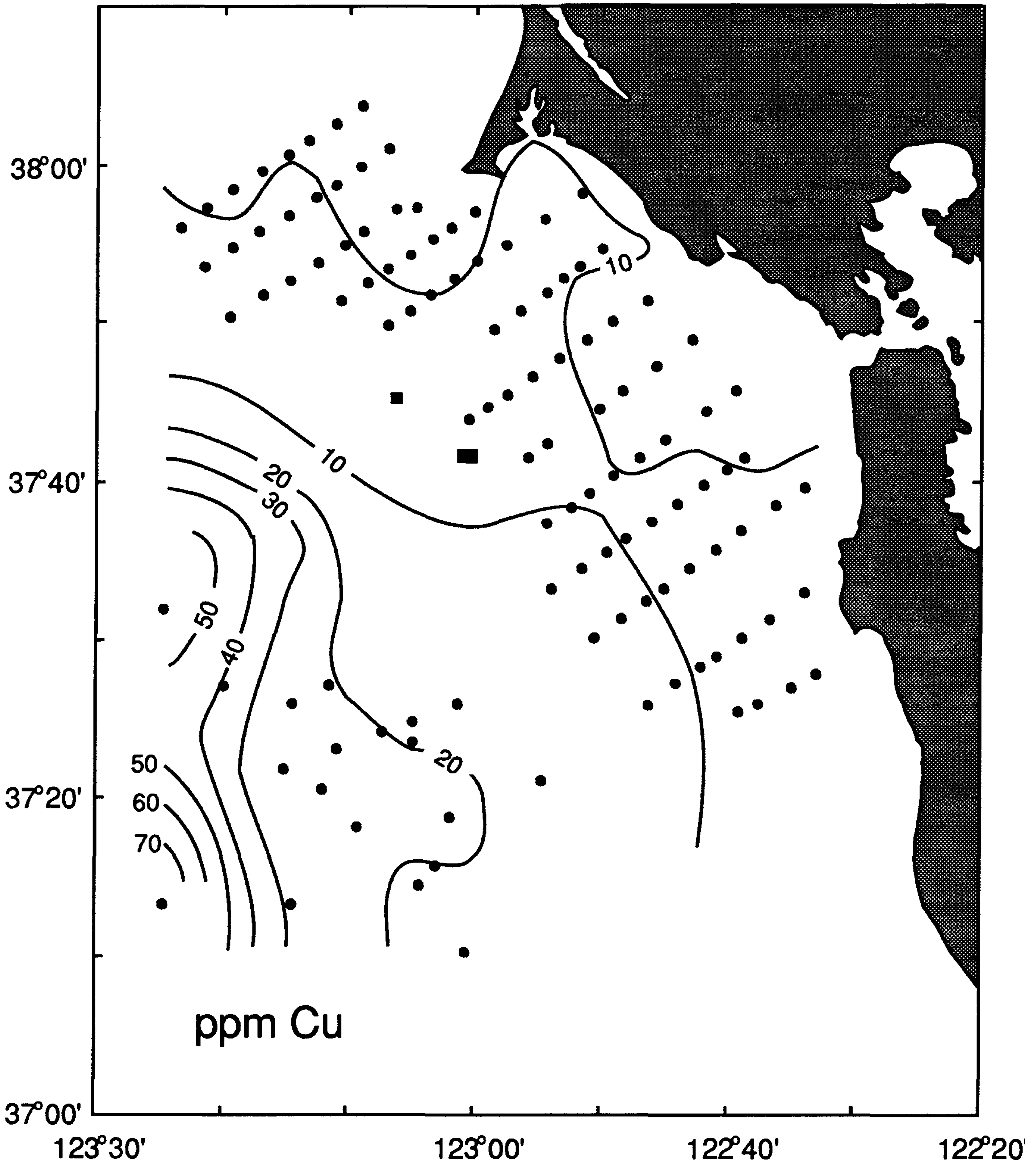

Figure 6E. Map of ppm Cu in surface sediments.

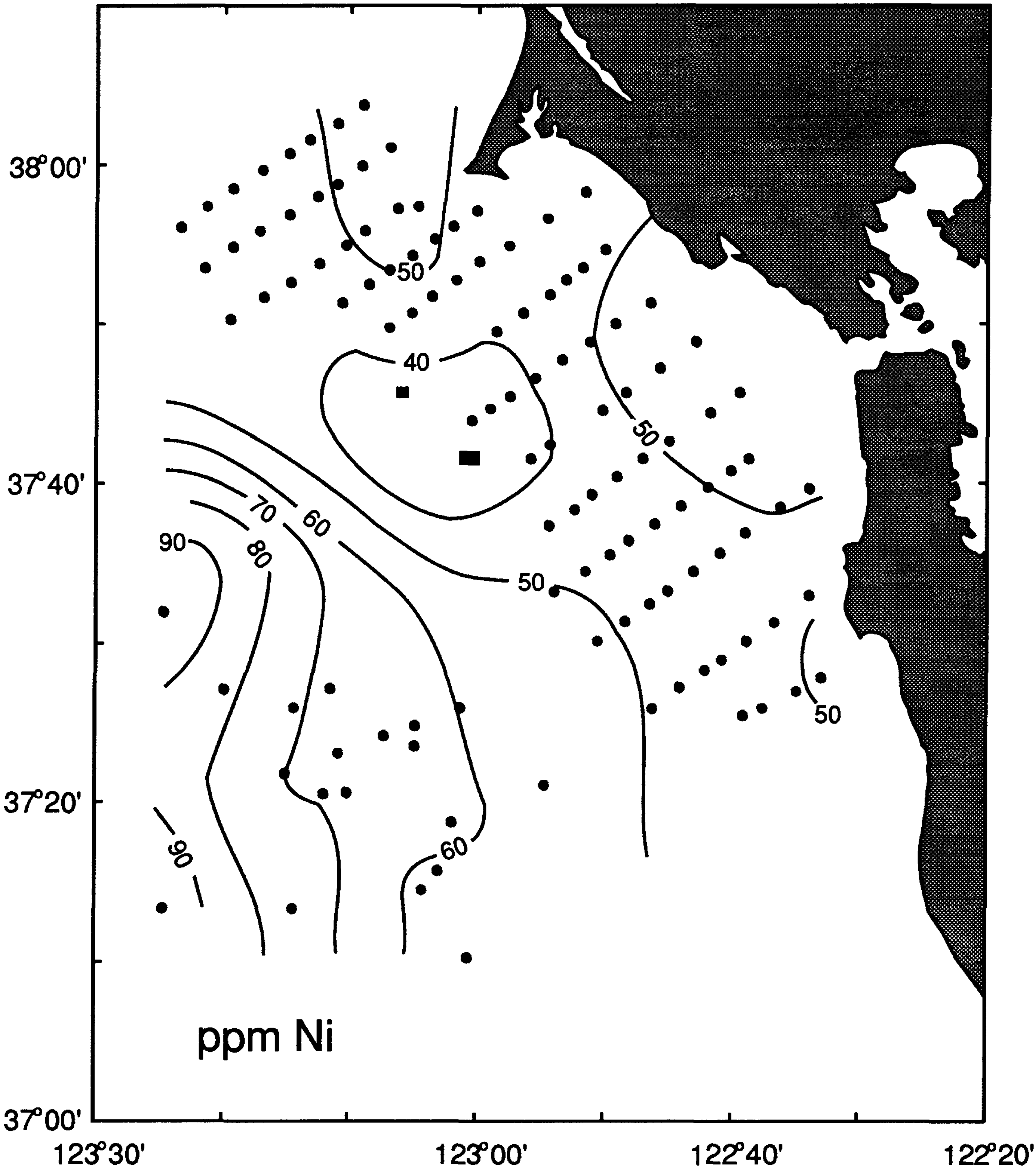

Figure 6F. Map of ppm Ni in surface sediments.

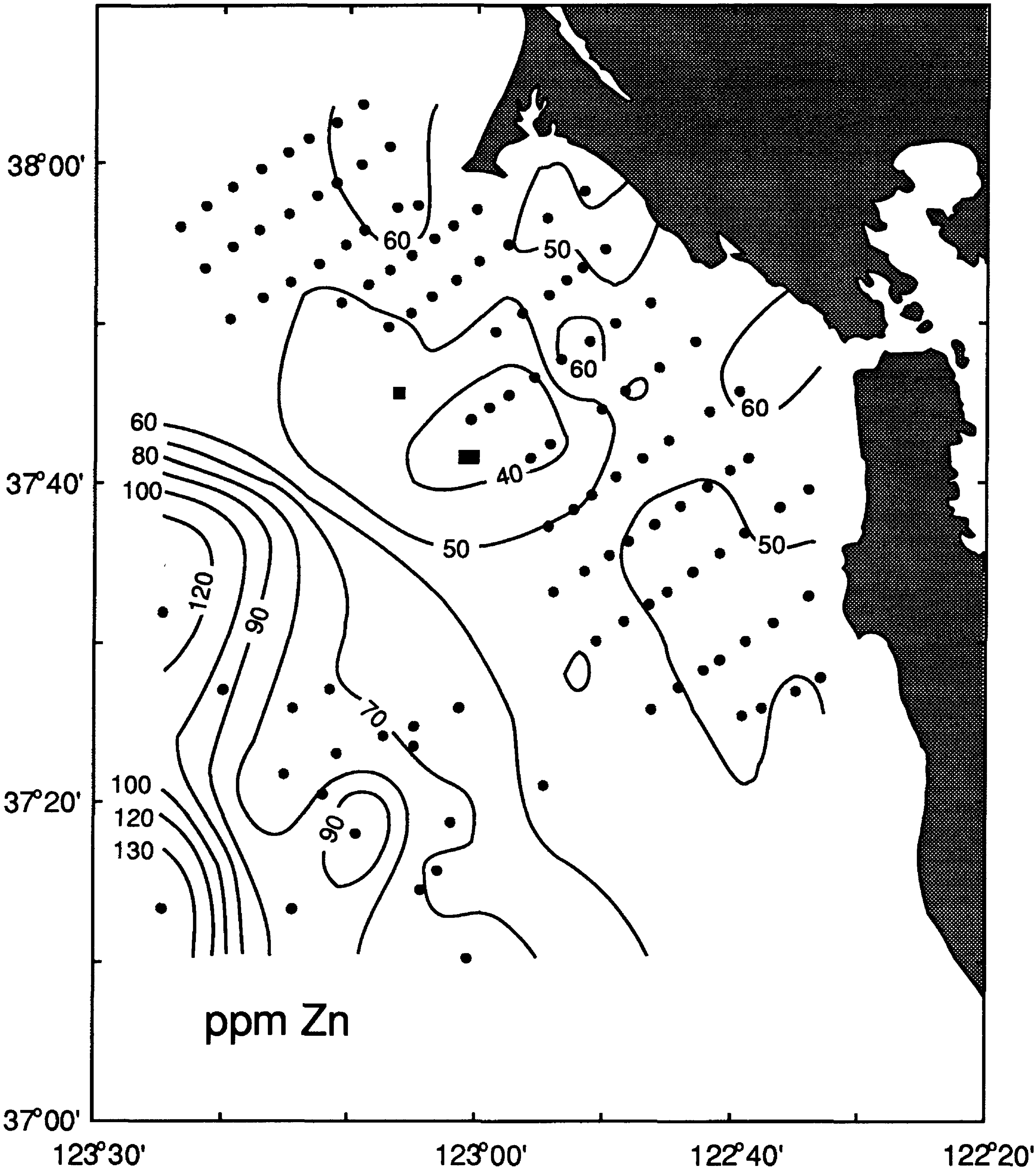

Figure 6G. Map of ppm Zn in surface sediments.

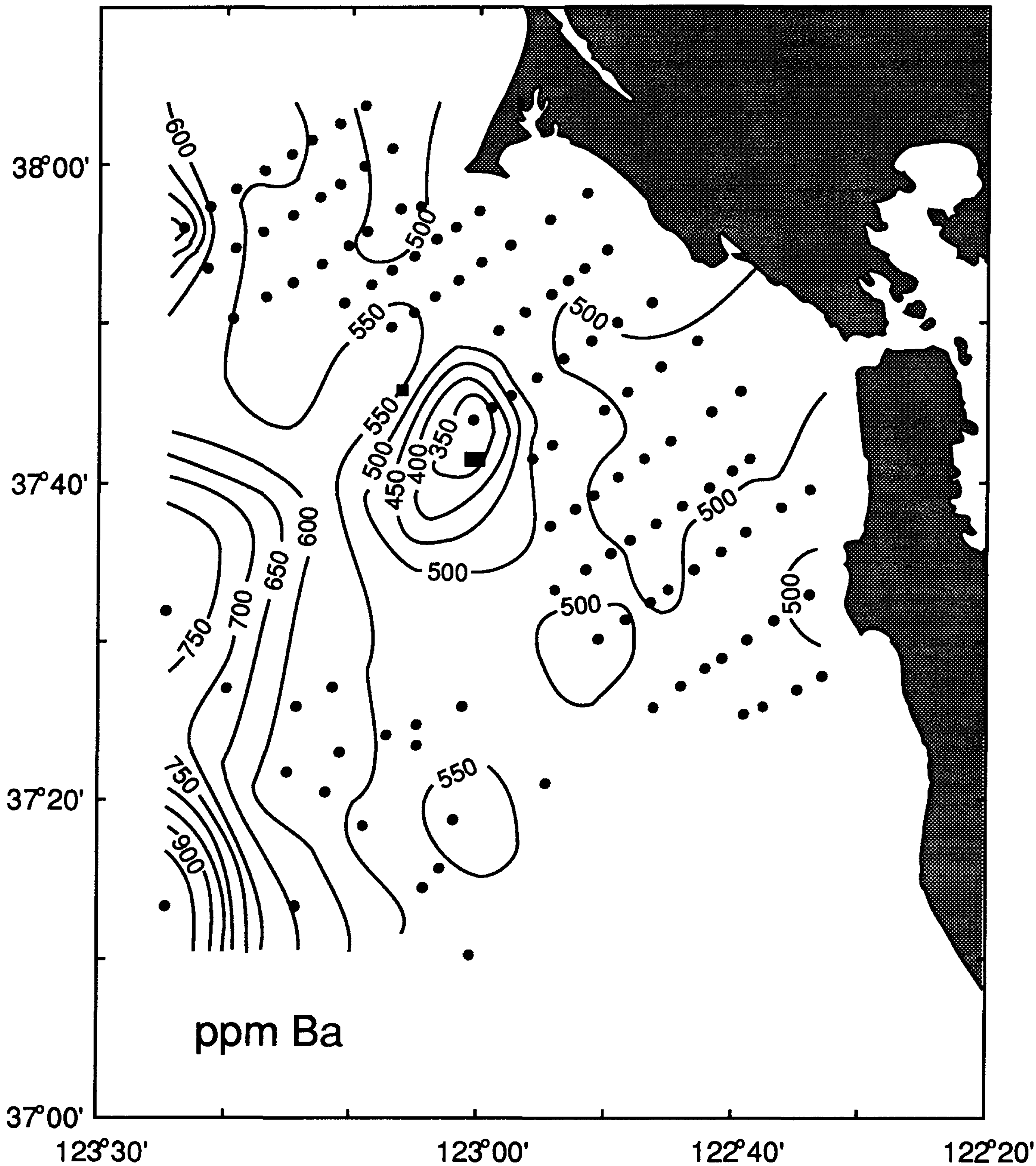

Figure 6H. Map of ppm Ba in surface sediments.

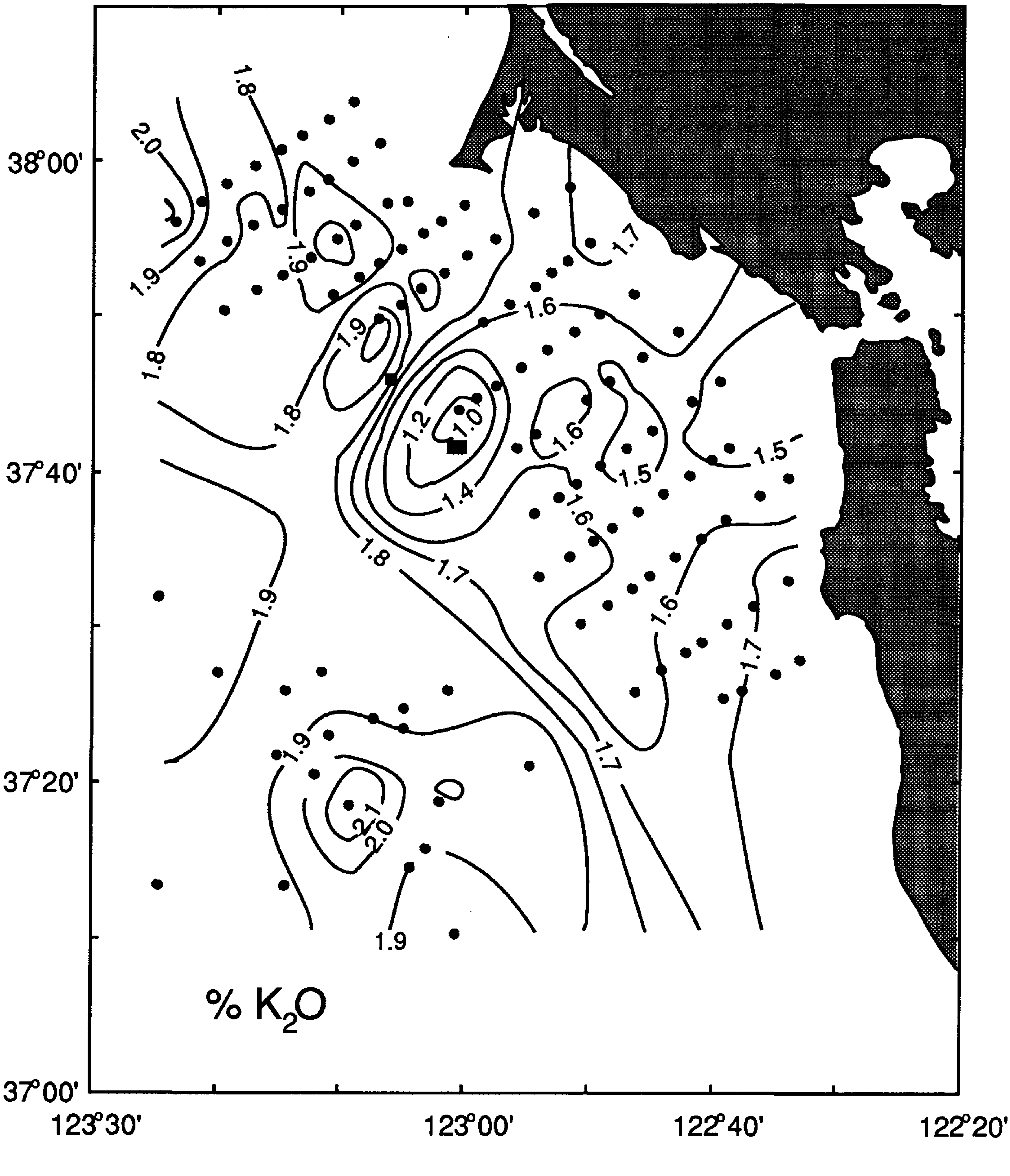

Figure 6I. Map of % K2O in surface sediments.

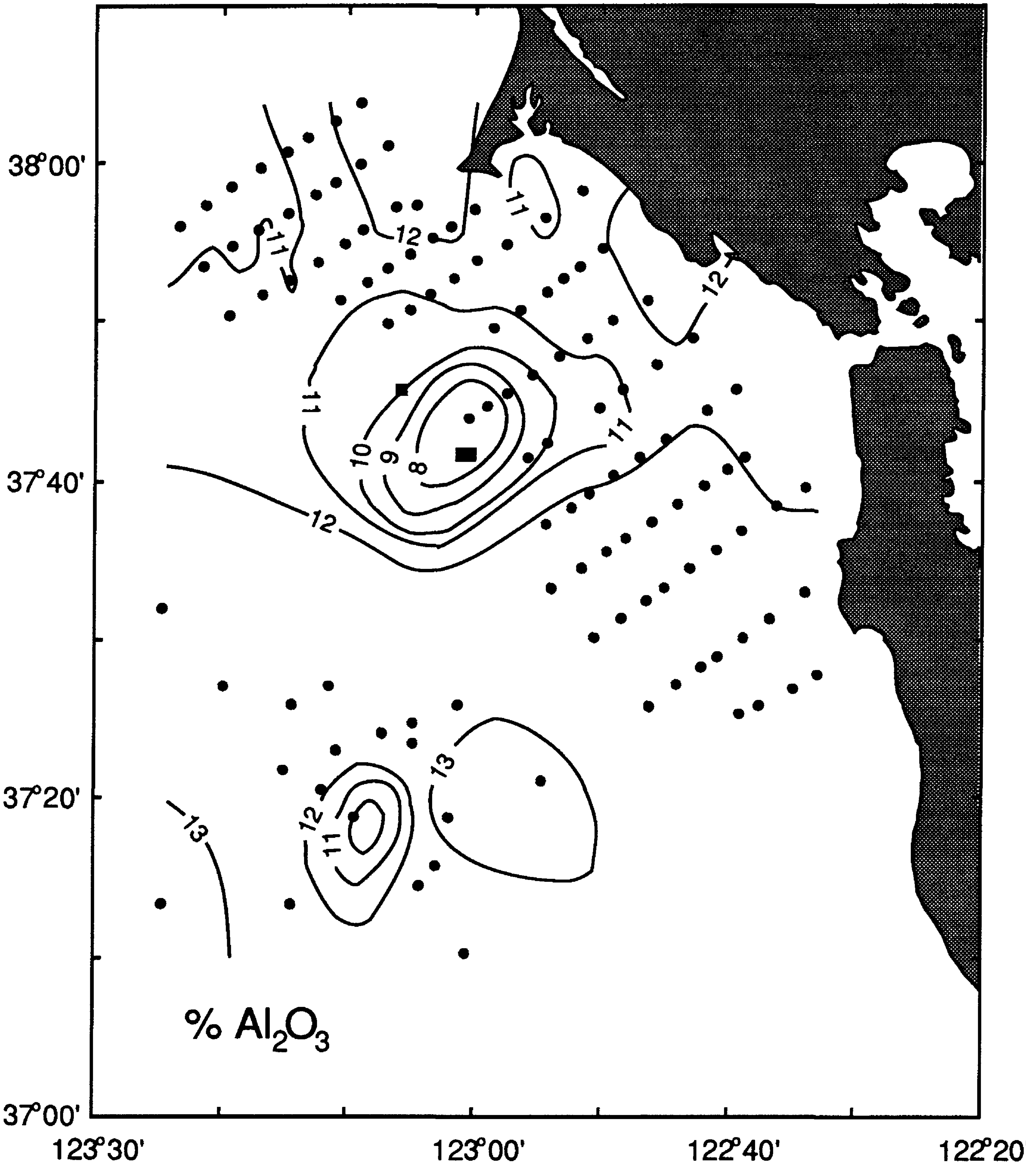

Figure 6J. Map of % Al2O3 in surface sediments.

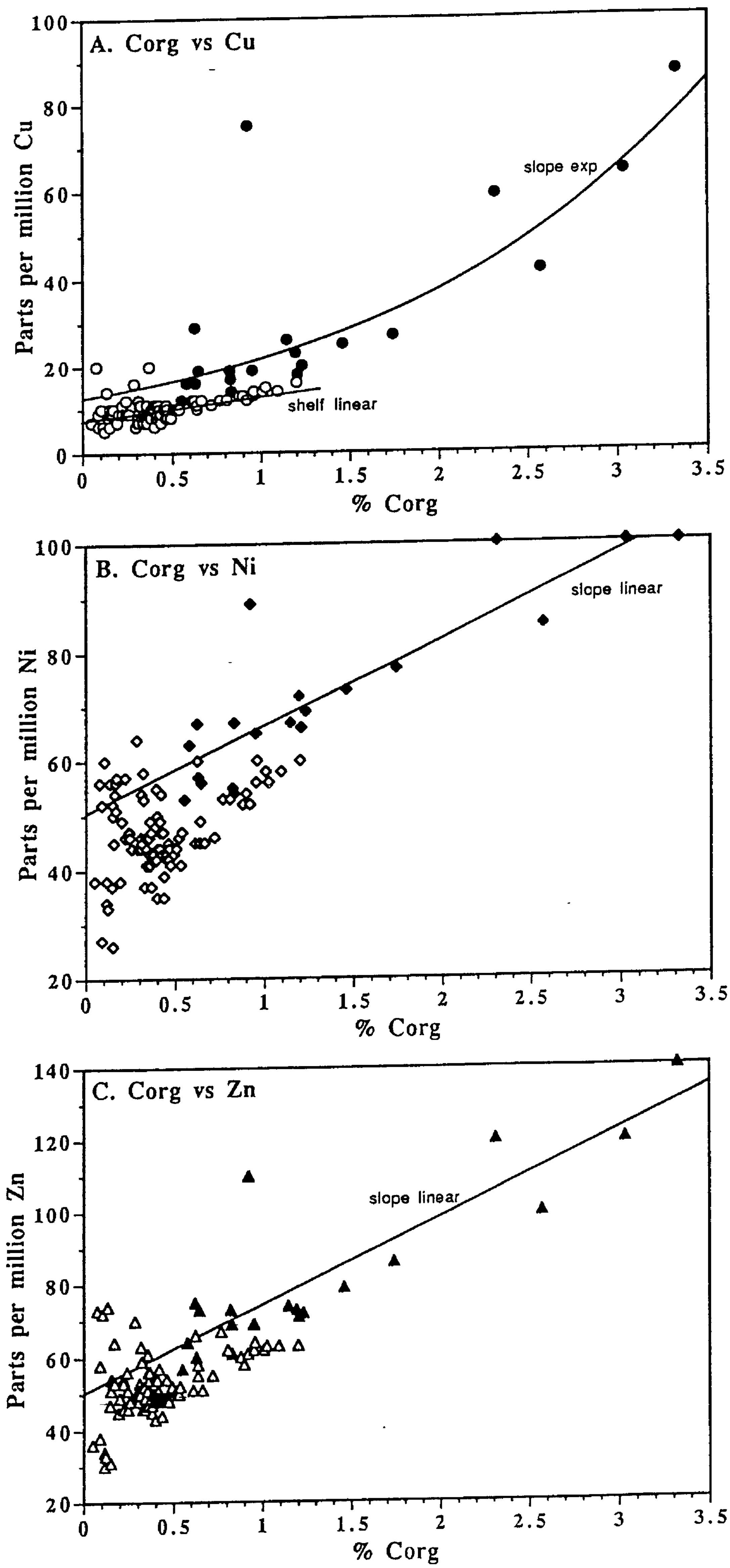

Figure 7. Scatter plot of %Corg versus ppm Cu (A), ppm Ni (B), and ppm Zn (C) in surface sediments in shelf (open symbols) and slope (solid symbols) cores from the Gulf of the Farallones.

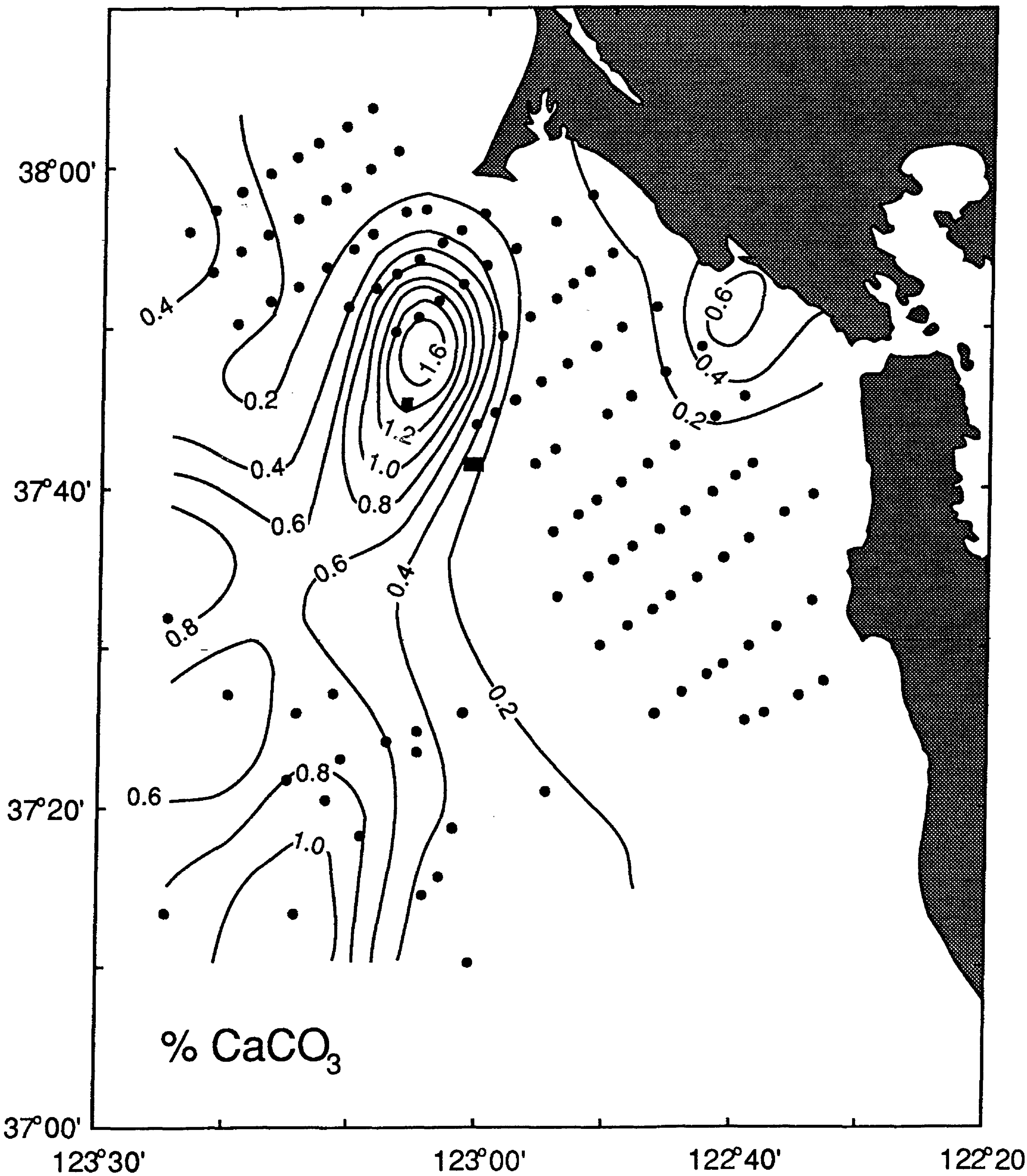

Figure 8. Maps of %CaCO3 (A) and ppm Sr (B) in surface sediments from the Gulf of the Farallones. Black solid rectangles indicate the locations of the Farallon Islands.

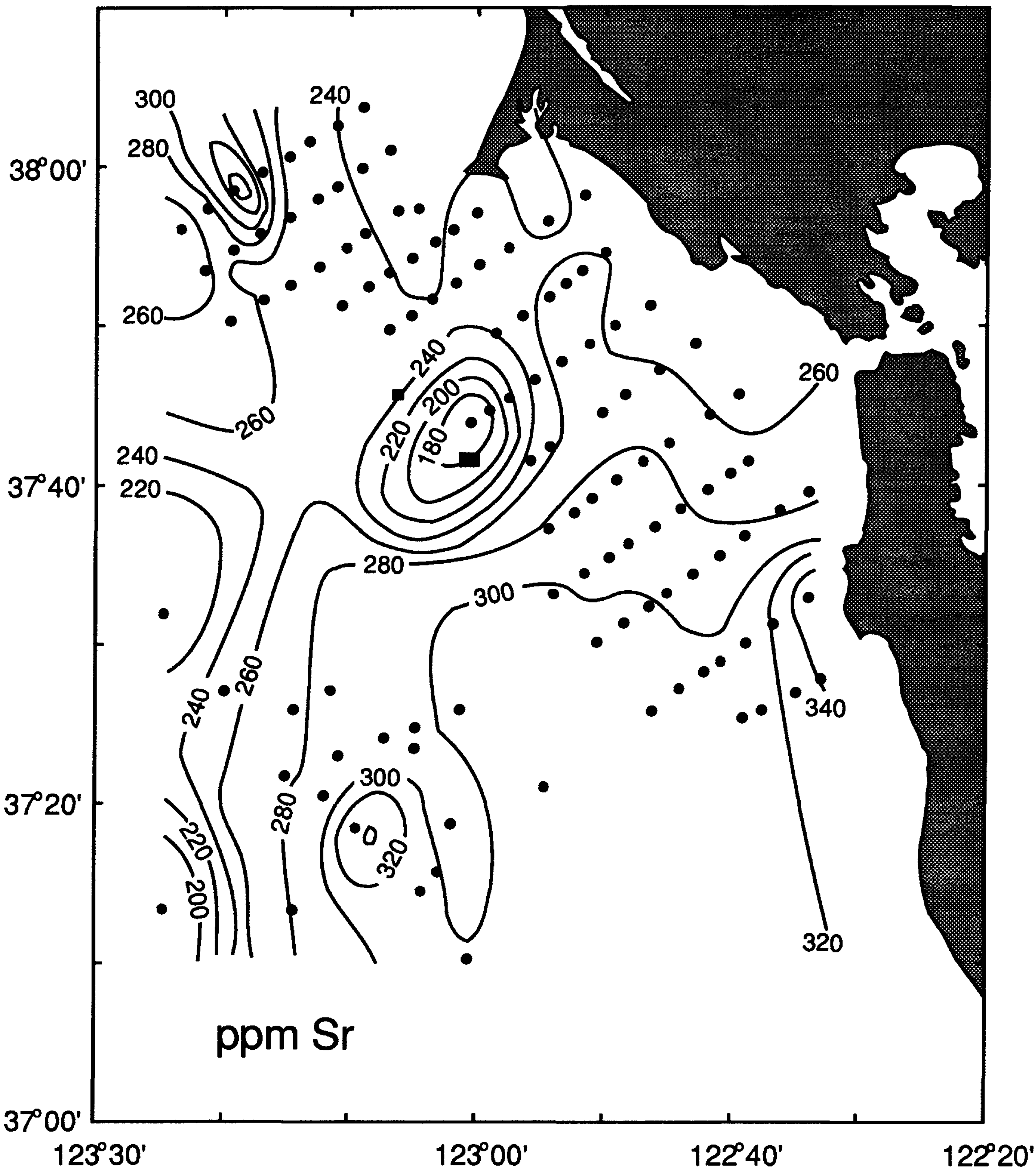

Figure 8B. Map of ppm Sr in surface sediments.

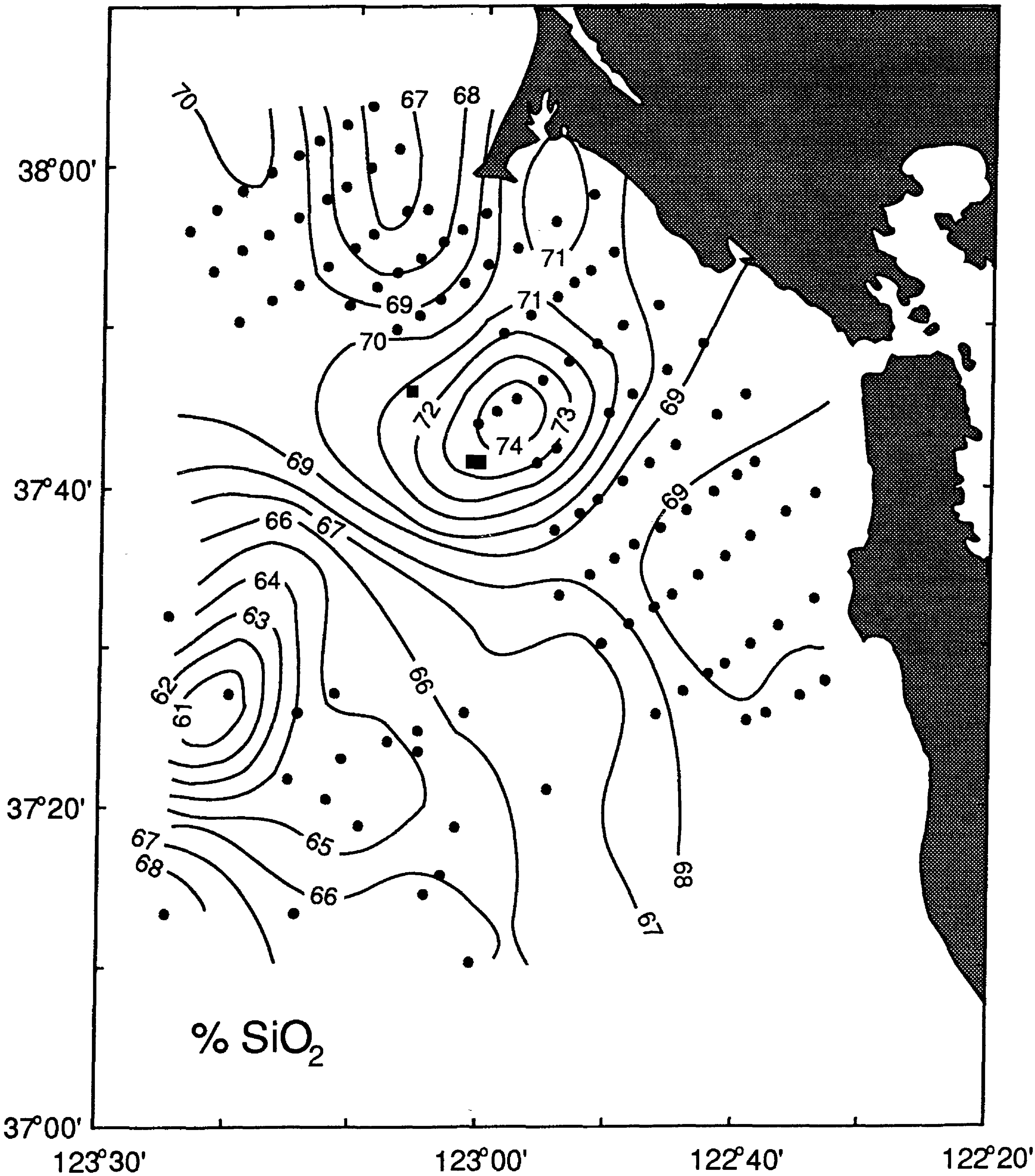

Figure 9. Map of %SiO_2 in surface sediments from the Gulf of the Farallones. Black solid rectangles indicate the locations of the Farallon Islands.

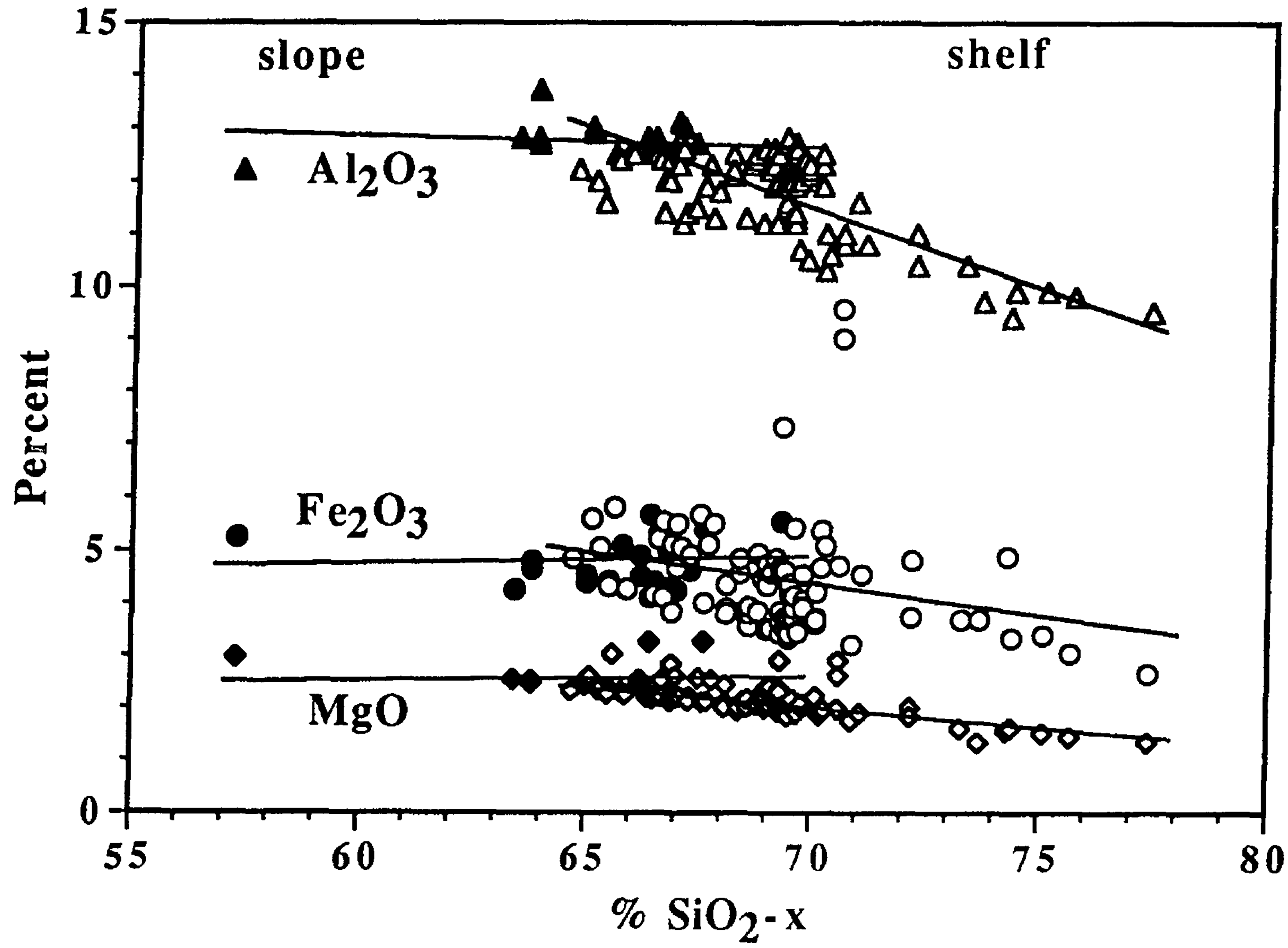

Figure 10. Scatter plot of %SiO_2 versus %Fe_2O_3 (circles), %MgO (diamonds), and %Al_2O_3 (triangles) in surface sediments in shelf (open symbols) and slope (solid symbols) cores from the Gulf of the Farallones. Lines through the slope and shelf data are linear regressions.

REFERENCES CITED

Baedecker, P.A. (Editor), 1987, Geochemical methods of analysis. U.S. Geological Survey Bulletin 1770, 129 p.

Brumsack, H.J., 1986, The inorganic geochemistry of Cretaceous black shales (DSDP Leg 41) in comparison to modern upwelling sediments from the Gulf of California, *in* Summerhayes, C.P., and Shackleton, N.J., eds., North Atlantic paleoceanography: Geological Society Special Publication No. 21, London, Blackwell Scientific Publications, p. 447-462.

Blake, M.C., Jr., Howell, D.G., and Jayko, A.S., 1984, Tectonostratigraphic terranes of the San Francisco Bay region, *in* Blake, M.C., Jr., ed., Franciscan geology of northern California: Pacific Section, Society of Economic Paleontologists and Mineralalogists, v. 43, p. 5-22.

Cacchione, D.A., Drake, D.E., Ferreira, J.T., and Tate, G.B., 1994, Bottom stress estimates and sand transport on northern California inner continental shelf: Continental Shelf Research, v. 14, p. 1273-1289.

California Division of Mines and Geology, 1980, Geologic map of California, San Francisco sheet, 1:250:000.

Conomos, T.J., 1979, Properties and circulation of San Francisco Bay waters, *in* Conomos, T.J., ed., San Francisco Bay: The urbanized estuary: Pacific Division American Association for the Advancement of Science, p. 47-84.

Engleman, E.E., Jackson, L.L., Norton, D. R., and Fischer, A.G., 1985, Determination of carbonate carbon in geological materials by coulometric titration: Chemical Geology, v. 53, p. 125-128.

Drake, D.E. and Cacchione, D.A., 1985, Seasonal variation in sediment transport on the Russian River shelf, California: Continental Shelf Research, v. 4, p. 495-514.

Dymond, J., Suess, E., and Lyle, M., 1992, Barium in deep-sea sediment: a geochemical proxy for paleoproductivity: Paleoceanography, v. 7, p. 163-181.

Hall, J.F., 1965, Petrology of the type Merced Group. San Francisco Peninsula, California (unpublished MA thesis): Univ. of Calif., Berkeley, 126p.

Hall, J.F., 1966, Fleishacker Zoo to Mussel Rock (Merced Formation)-A Plio-Pleistocene nature walk: Calif. Div. Mines Geol. Mineral. Info Service, v. 19, p. S22-S25.

Holland, H. D., 1979, Metals in black shales - a reassesment: Economic Geology, v. 74, p. 1676-1679.

Huyer, A., Kosro, P.M., Lentz, S., and Beardsley, R.C., 1989, Poleward flows in the California Current system, *in* Neshyba, S.J., Moores, C.N. K., Smith, R.L., and Barber, R.T., eds., Poleward flows along eastrern ocean boundaries: Springer-Verlag Coastal and Estuarine Studies, Vol. 34, 374 p.

Huyer, A., Kosro, P.M., Fleischbein, J., Ramp, S.R., Stanton, T., Washburn, L., Chavez, F.P., Cowles, T.J., Pierce, S.D., and Smith, R.L., 1991, Currents and water masses of the coastal transition zone off northern California, June to August, 1988: Journal of Geophysical Research, v. 96, p. 14,809-14,832.

Karl, H.A.., ed., 1992, Comprehensive geological and geophysical survey of the Gulf of the Farallones region: U. S. Geological Survey Administrative Report to the U. S. Environmental Protection Agency, 188 p.

Klovan, J.E., and Miesch, A.T., 1976, Extended CABFAC and QMODEL computer programs for Q-mode factor analysis of compositional data: Computers and Geosciences, v. 1, p.161-178.

Maher, N.M., Karl, H.A., Chin, J.L., and Schwab, W.C., 1991, Station locations and grain-size analysis of surficial sediment samples collected on the continental shelf, Gulf of the

Farallones during cruise F2-89-NC, January, 1989: U. S. Geological Survey Open-File Report 91-375-A, 42 p.

Miesch, A.T., 1981, Computer methods for geochemical and petrologic mixing problems, *in* Merriam, D.F., ed., Computer applications in the earth sciences: Plenum Publishing Corporation, p.244-265.

Noble, M., and Gelfenbaum, G., 1990, A pilot study of currents and suspended sediment in the Gulf of the Farallones: U. S. Geological Survey Open-File Report 90-476.

Noble, M., Ramp, S.R., and Kinoshita, K., 1992, Current patterns over the shelf and slope adjacent to the Gulf of the Farallones: Executive summary: U. S. Geological Survey Open-File Report 92-382, 26 p.

Ramp, S.R., Jessen, P.F., Brink, K. H., Niiler, P.P., Daggett, F.L., and Best, J.S., 1991, The physical structure of cold filaments near Point Arena, California, during June, 1987: Journal of Geophysical Research, v. 96, p. 14,859-14,884. 1991

Send, U., Beardsley, R.C., and Winant, C.D., 1987, Relaxation from upwelling in the Coastal Ocean Dynamics Experiment: Journal of Geophysical Research, v. 92, No. C2, p. 1683-1698.

Strub, P.T., Kosro, P.M., and Huyer, A., 1991, The nature of the cold filaments in the California Current system: Journal of Geophysical Research, v. 96, p. 14,743-14,768.

Vine, J.D., and Tourtelot, E.B., 1970, Geochemistry of black shales - a summary report: Economic Geology, v. 65, p. 253-272.

Wahrhaftig, C., 1984, A street car to subduction and other plate tectonic trips by public transport in San Francisco, revised edition: American Geophysical Union, 76 p.

Washburn, L., Swenson, M.S., Largier, J.L., Kosro, P.M., and Ramp, S.R., 1993, Cross-shelf sediment transport by an anticyclonic eddy off northern California: Science, v. 261, p. 1560-1564.

Appendix I. Concentrations of major elements in samples of sediment in cores from the continental shelf in the Gulf of the Farallones.

Core	Latitude	Longitude	Depth (in)	% SiO2-x	% Al2O3-x	% Al2O3-icp	% Fe2O3-x	% Fe2O3-icp	% MgO-x	% MgO-icp	% CaO-x	% CaO-icp	% Na2O-x	% Na2O-icp
F2-89-V01	37.935	-123.389	119	70.2	10.3	10.6	5.36	5.58	1.85	1.82	1.98	2.10	3.19	3.37
F2-89-V02	37.956	-123.354	104	67.0	11.2	11.3	5.49	5.58	2.19	2.16	2.00	2.10	3.28	3.37
F2-89-V03	37.974	-123.320	108	n.a.	n.a.	10.6	n.a.	4.86	n.a.	1.99	n.a.	7.27	n.a.	3.64
F2-89-V04	37.995	-123.283	113	71.1	10.8	11.1	4.54	4.58	1.89	1.82	1.72	1.82	3.34	3.50
F2-89-V05	38.012	-123.247	110	70.2	11.0	11.3	4.67	4.72	1.88	1.82	1.91	1.96	3.30	3.50
F2-89-V06	38.027	-123.220	108	68.4	11.3	11.9	4.56	4.58	1.93	1.99	2.39	2.38	3.18	3.50
F2-89-V07	38.043	-123.184	99	65.5	12.5	12.8	4.32	4.29	2.27	2.32	2.07	2.10	3.22	3.37
F2-89-V08	38.062	-123.151	84	66.7	12.4	12.7	4.10	4.15	2.21	2.16	2.16	2.24	3.48	3.64
F2-89-V09	37.892	-123.357	113	69.4	11.3	11.7	4.61	4.72	1.99	1.99	2.21	2.24	3.12	3.37
F2-89-V10	37.913	-123.320	106	70.3	10.6	11.0	5.08	5.15	1.95	1.99	2.00	2.10	3.24	3.37
F2-89-V11	37.930	-123.285	106	67.7	11.3	11.7	5.11	5.15	2.12	2.16	2.72	2.80	3.12	3.37
F2-89-V12	37.947	-123.246	102	69.6	10.7	11.0	5.40	5.43	2.01	1.99	1.90	1.96	3.30	3.37
F2-89-V13	37.966	-123.210	102	68.4	11.3	11.7	4.84	4.86	2.00	1.99	2.71	2.80	3.11	3.37
F2-89-V14	37.980	-123.184	102	67.3	11.5	11.7	4.91	5.01	2.13	2.16	2.00	2.10	3.35	3.50
F2-89-V15	37.998	-123.152	90	66.4	12.5	12.5	4.11	4.15	2.19	2.16	2.13	2.24	3.20	3.37
F2-89-V16	38.018	-123.114	73	67.6	12.3	12.5	4.01	4.00	2.11	1.99	2.12	2.10	3.39	3.50
F2-89-V17	37.837	-123.323	117	69.3	11.5	11.9	4.63	4.72	2.06	2.16	2.22	2.24	3.16	3.37
F2-89-V18	37.858	-123.280	102	68.8	11.2	11.7	4.94	5.15	2.07	2.16	2.46	2.52	3.15	3.37
F2-89-V19	37.877	-123.244	99	70.6	10.8	11.1	4.71	4.86	1.98	1.99	1.93	1.96	3.26	3.50
F2-89-V20	37.896	-123.207	95	69.1	11.2	11.7	4.58	4.58	2.03	1.99	2.70	2.66	3.20	3.37
F2-89-V21	37.915	-123.172	95	67.1	11.4	12.1	5.05	5.01	2.20	2.16	3.34	3.36	3.09	3.37
F2-89-V22	37.929	-123.147	95	64.7	12.2	12.5	4.84	4.72	2.32	2.32	2.25	2.24	3.09	3.24
F2-89-V23	37.954	-123.105	82	66.5	12.4	12.5	4.15	4.15	2.23	2.16	2.14	2.10	3.48	3.50
F2-89-V24	37.956	-123.077	76	65.9	12.5	12.8	4.27	4.15	2.25	2.16	2.16	2.10	3.17	3.37
F2-89-V25	37.829	-123.115	86	73.7	9.7	10.0	3.69	3.86	1.33	1.36	1.88	1.96	3.14	3.24
F2-89-V26	37.845	-123.086	88	65.3	11.6	12.1	5.05	5.15	2.35	2.49	3.19	3.36	3.06	3.37
F2-89-V27	37.861	-123.058	88	69.8	10.5	10.8	4.53	4.72	2.03	1.99	2.10	2.10	3.12	3.24
F2-89-V28	37.878	-123.027	84	68.1	12.1	12.5	3.91	4.00	2.10	1.99	2.52	2.52	3.26	3.37
F2-89-V29	37.897	-122.995	73	69.4	12.0	12.3	3.53	3.58	1.90	1.82	2.30	2.38	3.19	3.37
F2-89-V30	37.914	-122.959	64	70.9	11.6	11.9	3.21	3.29	1.75	1.82	2.28	2.38	3.38	3.50
F2-89-V31	37.943	-122.907	46	75.1	9.9	10.0	3.39	3.58	1.51	1.53	1.86	1.96	3.18	3.24
F2-89-V32	37.969	-122.858	38	69.3	12.1	12.3	3.85	3.86	1.93	1.99	2.38	2.38	3.03	3.24
F2-89-V33	37.826	-122.974	74	73.3	10.4	10.6	3.69	3.72	1.60	1.59	1.59	1.54	3.22	3.37
F2-89-V34	37.844	-122.939	68	69.5	11.3	11.9	4.19	4.43	1.95	1.99	2.36	2.52	3.36	3.64
F2-89-V36	37.878	-122.882	59	69.6	12.3	12.7	3.73	3.86	1.99	1.99	2.48	2.52	3.34	3.50
F2-89-V37	37.892	-122.861	53	69.6	12.1	12.7	3.91	4.00	2.02	1.99	2.42	2.38	3.14	3.37
F2-89-V38	37.911	-122.832	40	69.8	12.1	12.5	4.05	4.15	2.02	1.99	2.34	2.52	3.01	3.24
F2-89-V40	37.743	-122.983	58	n.a.	n.a.	5.3	n.a.	4.72	n.a.	1.29	n.a.	2.52	n.a.	1.48
F2-89-V41	37.757	-122.958	58	75.7	9.8	10.2	3.04	3.15	1.44	1.48	1.77	1.82	3.19	3.37
F2-89-V42	37.776	-122.924	59	77.4	9.5	9.8	2.65	2.86	1.34	1.39	1.67	1.82	2.89	3.10
F2-89-V43	37.795	-122.888	55	n.a.	n.a.	11.9	n.a.	7.29	n.a.	2.98	n.a.	4.34	n.a.	3.64
F2-89-V44	37.814	-122.852	53	n.a.	n.a.	11.3	n.a.	9.01	n.a.	2.98	n.a.	4.20	n.a.	3.10

[-x, analyzed by X-ray fluorecence; -icp, analyzed by ICP; LOI 925C, loss on ignition at 925 degrees C; n.a., not analyzed]

Appendix I. Concentrations of major elements in samples of sediment in cores from the continental shelf in the Gulf of the Farallones.

Core	Latitude	Longitude	Depth (m)	% SiO2-x	% Al2O3-x	% Al2O3-icp	% Fe2O3-x	% Fe2O3-icp	% MgO-x	% MgO-icp	% CaO-x	% CaO-icp	% Na2O-x	% Na2O-icp
F2-89-V45	37.833	-122.819	48	72.2	11.0	11.1	3.74	3.86	1.83	1.82	1.86	1.96	3.17	3.24
F2-89-V46	37.856	-122.772	40	69.0	12.3	12.7	4.34	4.58	2.21	2.32	2.51	2.66	3.00	3.24
F2-89-V47	37.691	-122.929	55	n.a.	n.a.	n.a.	n.a.	n.a.	n.a.	n.a.	n.a.	n.a.	n.a.	n.a.
F2-89-V48	37.706	-122.903	57	74.4	9.9	10.4	3.34	3.58	1.61	1.61	1.94	1.96	3.13	3.37
F2-89-V50	37.742	-122.834	53	74.3	9.4	9.6	4.88	5.01	1.55	1.58	2.17	2.24	2.75	2.97
F2-89-V51	37.762	-122.804	53	n.a.	n.a.	11.3	n.a.	9.58	n.a.	2.65	n.a.	3.78	n.a.	3.37
F2-89-V52	37.786	-122.760	42	68.9	12.2	12.7	4.47	4.58	2.27	2.32	2.61	2.66	3.03	3.24
F2-89-V53	37.814	-122.713	31	69.2	11.9	12.1	4.84	4.86	2.25	2.32	2.37	2.38	3.18	3.37
F2-89-V54	37.620	-122.905	82	69.5	12.3	12.5	3.32	3.43	1.95	1.99	2.61	2.66	3.50	3.64
F2-89-V55	37.638	-122.872	69	68.6	12.4	12.7	3.56	3.58	2.00	1.99	2.84	2.94	3.26	3.50
F2-89-V56	37.651	-122.847	62	68.5	12.3	12.8	3.85	3.86	2.13	2.16	2.95	2.94	3.29	3.50
F2-89-V57	37.671	-122.815	53	65.1	12.0	12.3	5.59	5.58	2.60	2.65	3.56	3.64	3.20	3.50
F2-89-V58	37.690	-122.782	51	66.6	12.0	12.3	5.33	5.15	2.44	2.49	3.54	3.50	3.11	3.37
F2-89-V59	37.708	-122.748	42	66.7	12.0	12.5	5.54	5.58	2.53	2.49	3.23	3.36	3.16	3.37
F2-89-V60	37.739	-122.694	33	69.3	12.0	12.3	4.66	4.72	2.37	2.32	2.68	2.80	3.15	3.37
F2-89-V61	37.761	-122.656	22	67.8	11.8	12.3	5.49	5.58	2.53	2.49	2.96	3.08	2.75	3.10
F2-89-V62	37.551	-122.898	99	67.0	12.6	12.8	4.67	4.72	2.60	2.49	3.42	3.50	3.09	3.37
F2-89-V63	37.572	-122.857	86	68.6	12.5	13.0	3.80	3.72	2.17	2.16	2.74	2.80	3.22	3.50
F2-89-V64	37.590	-122.825	73	69.1	12.5	12.8	3.52	3.72	2.04	2.16	2.81	2.94	3.30	3.50
F2-89-V65	37.603	-122.800	64	69.7	12.4	12.7	3.48	3.58	1.99	1.99	2.83	2.94	3.47	3.50
F2-89-V66	37.622	-122.765	53	70.1	12.3	12.7	3.61	3.72	1.96	1.99	2.90	2.94	3.28	3.50
F2-89-V67	37.641	-122.730	46	70.1	12.3	12.7	3.71	3.86	2.00	1.99	2.81	2.94	3.42	3.50
F2-89-V68	37.660	-122.696	38	69.8	12.2	12.7	3.94	4.00	2.08	2.16	2.70	2.66	3.16	3.37
F2-89-V69	37.678	-122.666	33	69.1	12.0	12.7	4.57	4.72	2.40	2.49	2.85	2.94	3.02	3.37
F2-89-V70	37.691	-122.644	29	69.0	11.9	12.5	4.74	4.86	2.38	2.49	2.92	2.94	2.99	3.24
F2-89-V71	37.501	-122.840	91	65.6	12.4	12.7	5.81	5.72	3.03	2.98	3.94	3.92	2.95	3.24
F2-89-V72	37.520	-122.805	86	68.1	12.5	13.0	4.35	4.43	2.44	2.49	3.30	3.36	3.10	3.37
F2-89-V73	37.539	-122.772	73	69.5	12.6	13.0	3.42	3.58	1.99	1.99	2.87	2.94	3.26	3.50
F2-89-V74	37.553	-122.749	66	69.5	12.5	12.8	3.53	3.58	2.03	1.99	2.88	2.94	3.45	3.50
F2-89-V75	37.573	-122.715	55	69.7	12.4	13.0	3.44	3.58	1.88	1.99	2.69	2.94	3.28	3.50
F2-89-V76	37.592	-122.681	66	70.1	12.5	12.8	3.68	3.72	2.01	1.99	2.71	2.80	3.40	3.50
F2-89-V77	37.612	-122.648	38	69.8	12.3	12.7	3.91	4.00	2.06	2.16	2.65	2.66	3.14	3.37
F2-89-V78	37.639	-122.602	29	69.3	11.9	12.3	4.60	4.72	2.30	2.32	2.99	3.08	3.21	3.37
F2-89-V79	37.658	-122.564	25	70.1	11.9	12.3	4.21	4.43	2.21	2.32	2.86	2.94	3.03	3.24
F2-89-V80	37.429	-122.768	88	66.9	12.5	12.8	5.10	5.29	2.84	2.82	3.84	3.92	2.96	3.24
F2-89-V81	37.452	-122.733	81	68.6	12.5	13.0	3.93	3.86	2.17	2.16	3.12	3.08	3.20	3.50
F2-89-V82	37.470	-122.701	73	69.5	12.7	13.0	3.47	3.58	2.03	1.99	2.89	2.94	3.27	3.50
F2-89-V83	37.480	-122.679	68	69.3	12.7	12.8	3.42	3.43	2.01	1.99	2.86	2.94	3.44	3.50
F2-89-V84	37.500	-122.642	59	69.5	12.6	12.8	3.41	3.29	1.93	1.99	2.86	2.80	3.29	3.50
F2-89-V85	37.521	-122.610	51	68.8	12.6	13.0	3.85	3.86	2.08	2.16	3.09	3.22	3.38	3.50
F2-89-V86	37.547	-122.565	35	69.3	12.8	13.2	3.65	3.72	1.92	1.99	3.26	3.36	3.13	3.37
F2-89-V87	37.421	-122.650	82	69.0	12.6	13.0	3.49	3.58	1.98	1.99	2.89	2.94	3.32	3.50

[-x, analyzed by X-ray fluorecence; -icp, analyzed by ICP; LOI 925C, loss on ignition at 925 degrees C; n.a., not analyzed]

Appendix I. Concentrations of major elements in samples of sediment in cores from the continental shelf in the Gulf of the Farallones.

Core	Latitude	Longitude	Depth (m)	% SiO2-x	% Al2O3-x	% Al2O3-icp	% Fe2O3-x	% Fe2O3-icp	% MgO-x	% MgO-icp	% CaO-x	% CaO-icp	% Na2O-x	% Na2O-icp
F2-89-V88	37.429	-122.626	69	69.4	12.4	12.7	3.73	3.86	2.05	1.99	2.96	2.94	3.33	3.50
F2-89-V89	37.446	-122.582	58	67.5	11.9	12.3	5.67	5.72	2.57	2.65	3.51	3.64	3.27	3.37
F2-89-V90	37.462	-122.548	45	69.6	12.0	12.3	4.14	4.15	2.16	2.16	3.57	3.64	3.15	3.24
F2-89-V91	37.855	-123.177	95	69.5	11.2	11.3	4.37	4.29	1.96	1.99	2.30	2.38	3.20	3.37
F2-89-V92	37.875	-123.142	93	66.6	11.4	11.9	5.20	5.15	2.23	2.16	3.21	3.36	3.09	3.37
F2-89-V94	37.905	-123.085	88	69.5	11.4	11.5	3.78	3.86	1.98	1.99	1.97	1.96	3.28	3.37
F2-89-V95	37.921	-123.055	77	66.9	12.3	12.7	3.83	3.86	2.12	2.16	2.21	2.24	3.24	3.50
F2-89-V96	37.935	-123.032	66	68.1	12.2	12.5	3.80	3.72	2.00	1.99	2.51	2.52	3.21	3.50
F2-89-V97	37.952	-123.000	58	69.5	11.9	12.1	3.70	3.72	1.83	1.82	2.21	2.24	3.28	3.37

[-x, analyzed by X-ray fluorescence; -icp, analyzed by ICP; LOI 925C, loss on ignition at 925 degrees C; n.a., not analyzed]

Appendix I. Concentrations of major elements in samples of sediment in cores from the continental shelf in the Gulf of the Farallones.

Core	% K2O-x	% K2O-icp	% TiO2-x	% TiO2-icp	% P2O5-x	% P2O5-icp	% MnO-x	% MnO-icp	% LOI 925C	% Total C	% Inorganic C	% Organic C	% CaCO3
F2-89-V01	2.24	2.28	0.440	0.434	0.130	0.137	0.020	0.031	3.69	0.51	0.11	0.40	0.89
F2-89-V02	1.89	1.92	0.680	0.634	0.180	0.183	0.030	0.043	5.43	0.95	0.03	0.92	0.22
F2-89-V03	n.a.	1.80	n.a.	0.667	n.a.	0.137	n.a.	0.048	n.a.	2.94	2.57	0.37	21.35
F2-89-V04	1.89	1.92	0.560	0.534	0.120	0.115	0.030	0.037	3.20	0.32	0.02	0.31	0.13
F2-89-V05	1.81	1.80	0.720	0.684	0.130	0.137	0.040	0.046	3.25	0.37	0.02	0.36	0.12
F2-89-V06	1.62	1.68	0.960	0.851	0.170	0.137	0.050	0.057	4.16	0.51	0.02	0.49	0.14
F2-89-V07	1.73	1.80	0.610	0.567	0.180	0.183	0.030	0.039	6.88	1.23	0.03	1.20	0.27
F2-89-V08	1.76	1.68	0.590	0.550	0.160	0.160	0.030	0.039	5.78	0.98	0.02	0.95	0.20
F2-89-V09	1.73	1.80	0.770	0.751	0.130	0.137	0.040	0.052	3.80	0.38	0.03	0.35	0.22
F2-89-V10	1.93	2.04	0.570	0.534	0.120	0.115	0.030	0.039	3.36	0.41	0.07	0.34	0.59
F2-89-V11	1.63	1.68	1.120	1.101	0.160	0.160	0.060	0.067	3.90	0.35	0.01	0.34	0.11
F2-89-V12	1.97	2.04	0.710	0.667	0.130	0.137	0.040	0.044	3.30	0.31	0.01	0.29	0.12
F2-89-V13	1.56	1.56	1.180	1.051	0.170	0.160	0.060	0.070	3.83	0.43	0.02	0.42	0.15
F2-89-V14	1.81	1.80	0.700	0.667	0.160	0.160	0.040	0.045	5.10	0.78	0.01	0.77	0.11
F2-89-V15	1.73	1.68	0.590	0.550	0.160	0.160	0.030	0.039	6.19	1.12	0.03	1.09	0.21
F2-89-V16	1.81	1.80	0.580	0.534	0.150	0.160	0.030	0.039	5.35	0.90	0.02	0.88	0.14
F2-89-V17	1.77	1.80	0.620	0.600	0.140	0.137	0.040	0.044	3.94	0.26	0.02	0.24	0.14
F2-89-V18	1.69	1.68	0.840	0.784	0.150	0.160	0.050	0.053	3.97	0.33	0.02	0.31	0.20
F2-89-V19	1.87	1.92	0.590	0.567	0.130	0.137	0.030	0.040	3.35	0.43	0.02	0.41	0.17
F2-89-V20	1.55	1.68	1.020	0.951	0.160	0.160	0.050	0.059	3.61	0.33	0.02	0.31	0.14
F2-89-V21	1.44	1.56	1.460	1.168	0.200	0.115	0.080	0.081	3.54	0.38	0.01	0.37	0.08
F2-89-V22	1.70	1.80	0.860	0.817	0.180	0.183	0.040	0.052	6.83	0.97	0.01	0.96	0.10
F2-89-V23	1.75	1.80	0.600	0.550	0.170	0.183	0.030	0.039	5.81	1.03	0.02	1.01	0.20
F2-89-V24	1.74	1.80	0.640	0.584	0.170	0.183	0.030	0.039	6.59	1.08	0.05	1.03	0.43
F2-89-V25	2.30	2.28	0.330	0.334	0.110	0.115	0.014	0.027	3.00	0.25	0.10	0.15	0.79
F2-89-V26	1.62	1.68	1.000	0.951	0.190	0.206	0.060	0.062	5.64	1.17	0.54	0.63	4.51
F2-89-V27	1.97	1.92	0.500	0.467	0.200	0.206	0.030	0.036	4.56	0.78	0.36	0.42	3.00
F2-89-V28	1.68	1.68	0.740	0.684	0.180	0.183	0.040	0.046	4.78	0.65	0.01	0.64	0.11
F2-89-V29	1.74	1.68	0.580	0.550	0.160	0.160	0.030	0.039	4.42	0.73	0.01	0.72	0.10
F2-89-V30	1.74	1.68	0.530	0.500	0.130	0.137	0.030	0.039	3.25	0.49	0.01	0.48	0.10
F2-89-V31	1.59	1.68	0.530	0.534	0.100	0.092	0.030	0.043	2.69	0.45	0.01	0.44	0.08
F2-89-V32	1.72	1.68	0.610	0.517	0.170	0.183	0.030	0.039	4.16	0.65	0.03	0.61	0.27
F2-89-V33	1.80	1.80	0.480	0.434	0.110	0.115	0.030	0.032	2.94	0.34	0.01	0.33	0.07
F2-89-V34	1.65	1.68	0.790	0.767	0.140	0.137	0.050	0.057	3.70	0.32	0.01	0.31	0.04
F2-89-V36	1.66	1.68	0.530	0.500	0.130	0.137	0.030	0.040	3.70	0.25	0.01	0.24	0.05
F2-89-V37	1.69	1.80	0.520	0.484	0.120	0.137	0.030	0.040	3.59	0.44	0.03	0.42	0.21
F2-89-V38	1.76	1.68	0.500	0.484	0.130	0.137	0.030	0.040	3.62	0.46	0.03	0.43	0.22
F2-89-V40	n.a.	0.56	n.a.	2.002	n.a.	0.092	n.a.	0.168	n.a.	0.11	0.02	0.09	0.20
F2-89-V41	1.55	1.56	0.410	0.417	0.100	0.115	0.030	0.036	2.04	0.13	0.01	0.12	0.05
F2-89-V42	1.67	1.68	0.280	0.300	0.090	0.092	0.020	0.031	1.80	0.12	0.00	0.12	0.02
F2-89-V43	n.a.	1.44	n.a.	1.668	n.a.	0.183	n.a.	0.125	n.a.	0.12	0.02	0.10	0.14
F2-89-V44	n.a.	1.44	n.a.	2.669	n.a.	0.206	n.a.	0.181	n.a.	0.14	0.00	0.13	0.03

[-x, analyzed by X-ray fluorecence; -icp, analyzed by ICP; LOI 925C, loss on ignition at 925 degrees C; n.a., not analyzed]

Appendix I. Concentrations of major elements in samples of sediment in cores from the continental shelf in the Gulf of the Farallones.

Core	% K2O-x	% K2O-icp	% TiO2-x	% TiO2-icp	% P2O5-x	% P2O5-icp	% MnO-x	% MnO-icp	% LOI 925C	% Total C	% Inorganic C	% Organic C	% CaCO3
F2-89-V45	1.74	1.68	0.410	0.400	0.110	0.115	0.020	0.034	3.21	0.41	0.01	0.40	0.08
F2-89-V46	1.64	1.56	0.570	0.567	0.140	0.137	0.040	0.046	3.48	0.41	0.02	0.39	0.16
F2-89-V47	n.a.	n.a.	n.a.	n.a.	n.a.	n.a.	n.a.	n.a.	n.a.	0.43	0.24	0.19	1.97
F2-89-V48	1.65	1.68	0.380	0.400	0.100	0.115	0.030	0.037	2.20	0.12	0.01	0.12	0.05
F2-89-V50	1.76	1.80	0.530	0.517	0.090	0.092	0.040	0.050	1.76	0.05	0.00	0.05	0.02
F2-89-V51	n.a.	1.32	n.a.	2.168	n.a.	0.183	n.a.	0.168	n.a.	0.09	0.01	0.08	0.10
F2-89-V52	1.62	1.68	0.620	0.550	0.130	0.137	0.040	0.048	3.29	0.33	0.02	0.31	0.12
F2-89-V53	1.70	1.68	0.570	0.517	0.140	0.137	0.040	0.045	3.26	0.37	0.15	0.22	1.25
F2-89-V54	1.66	1.56	0.510	0.467	0.140	0.137	0.030	0.040	3.92	0.68	0.01	0.67	0.11
F2-89-V55	1.58	1.56	0.630	0.584	0.140	0.137	0.040	0.046	4.03	0.51	0.01	0.51	0.04
F2-89-V56	1.54	1.56	0.760	0.701	0.160	0.160	0.050	0.053	3.69	0.40	0.00	0.40	0.03
F2-89-V57	1.44	1.44	1.480	1.418	0.180	0.183	0.100	0.107	3.36	0.18	0.01	0.17	0.07
F2-89-V58	1.43	1.44	1.300	1.234	0.160	0.160	0.090	0.092	3.06	0.22	0.00	0.22	0.02
F2-89-V59	1.46	1.44	1.000	0.901	0.160	0.160	0.070	0.076	3.15	0.09	0.00	0.09	0.02
F2-89-V60	1.54	1.56	0.660	0.600	0.130	0.137	0.040	0.054	2.78	0.18	0.01	0.17	0.09
F2-89-V61	1.42	1.44	0.910	0.784	0.150	0.137	0.070	0.075	3.48	0.30	0.02	0.29	0.14
F2-89-V62	1.64	1.68	0.720	0.684	0.150	0.160	0.060	0.063	3.43	0.42	0.00	0.42	0.02
F2-89-V63	1.67	1.80	0.560	0.550	0.140	0.137	0.040	0.045	3.74	0.54	0.01	0.54	0.04
F2-89-V64	1.60	1.56	0.570	0.534	0.140	0.137	0.040	0.045	3.57	0.53	0.01	0.52	0.07
F2-89-V65	1.58	1.56	0.570	0.517	0.140	0.137	0.040	0.044	3.23	0.48	0.01	0.47	0.12
F2-89-V66	1.52	1.56	0.620	0.534	0.140	0.137	0.040	0.045	3.03	0.36	0.01	0.34	0.12
F2-89-V67	1.56	1.56	0.580	0.517	0.120	0.115	0.040	0.045	2.78	0.26	0.01	0.26	0.04
F2-89-V68	1.52	1.56	0.590	0.500	0.140	0.137	0.040	0.045	2.91	0.23	0.01	0.22	0.07
F2-89-V69	1.47	1.44	0.670	0.600	0.130	0.137	0.050	0.057	2.96	0.18	0.01	0.17	0.10
F2-89-V70	1.46	1.56	0.770	0.651	0.140	0.137	0.050	0.059	2.91	0.17	0.01	0.16	0.10
F2-89-V71	1.53	1.56	0.950	0.867	0.160	0.160	0.080	0.081	2.97	0.32	0.00	0.32	0.03
F2-89-V72	1.61	1.68	0.690	0.667	0.140	0.137	0.050	0.061	3.19	0.41	0.00	0.41	0.02
F2-89-V73	1.58	1.56	0.510	0.500	0.120	0.115	0.040	0.044	3.38	0.48	0.01	0.47	0.05
F2-89-V74	1.59	1.56	0.530	0.484	0.130	0.137	0.030	0.044	3.33	0.44	0.01	0.43	0.10
F2-89-V75	1.57	1.56	0.540	0.534	0.130	0.137	0.030	0.041	3.08	0.40	0.01	0.38	0.12
F2-89-V76	1.61	1.68	0.570	0.517	0.140	0.137	0.030	0.043	2.80	0.26	0.01	0.25	0.12
F2-89-V77	1.62	1.68	0.600	0.534	0.140	0.137	0.040	0.045	2.99	0.22	0.02	0.20	0.17
F2-89-V78	1.51	1.44	0.810	0.701	0.150	0.137	0.050	0.061	2.54	0.17	0.02	0.15	0.16
F2-89-V79	1.51	1.44	0.670	0.600	0.140	0.137	0.050	0.054	2.71	0.17	0.02	0.15	0.13
F2-89-V80	1.53	1.56	0.790	0.767	0.140	0.137	0.070	0.077	2.72	0.33	0.01	0.32	0.05
F2-89-V81	1.62	1.68	0.590	0.567	0.130	0.137	0.040	0.052	3.07	0.39	0.01	0.38	0.07
F2-89-V82	1.64	1.68	0.520	0.500	0.130	0.137	0.040	0.044	3.46	0.46	0.01	0.45	0.06
F2-89-V83	1.62	1.56	0.540	0.500	0.130	0.137	0.030	0.043	3.25	0.47	0.01	0.46	0.07
F2-89-V84	1.64	1.68	0.560	0.500	0.130	0.137	0.040	0.040	3.29	0.45	0.01	0.44	0.08
F2-89-V85	1.71	1.80	0.620	0.600	0.130	0.137	0.040	0.048	3.02	0.39	0.01	0.37	0.11
F2-89-V86	1.79	1.80	0.620	0.584	0.160	0.160	0.040	0.045	2.68	0.22	0.03	0.19	0.22
F2-89-V87	1.67	1.68	0.530	0.500	0.130	0.137	0.040	0.044	3.68	0.54	0.01	0.53	0.08

[-x, analyzed by X-ray fluorecence; -icp, analyzed by ICP; LOI 925C, loss on ignition at 925 degrees C; n.a., not analyzed]

Appendix I. Concentrations of major elements in samples of sediment in cores from the continental shelf in the Gulf of the Farallones.

Core	% K2O-x	% K2O-icp	% TiO2-x	% TiO2-icp	% P2O5-x	% P2O5-icp	% MnO-x	% MnO-icp	% LOI 925C	% Total C	% Inorganic C	% Organic C	% CaCO3
F2-89-V88	1.75	1.80	0.590	0.567	0.130	0.137	0.040	0.050	3.02	0.47	0.01	0.46	0.06
F2-89-V89	1.75	1.80	0.830	0.801	0.130	0.137	0.070	0.079	2.36	0.16	0.01	0.16	0.04
F2-89-V90	1.70	1.68	0.820	0.734	0.150	0.137	0.060	0.065	2.07	0.15	0.01	0.15	0.05
F2-89-V91	1.63	1.68	0.770	0.717	0.140	0.137	0.040	0.048	3.86	0.38	0.02	0.36	0.15
F2-89-V92	1.50	1.56	1.400	1.218	0.190	0.160	0.070	0.079	3.93	0.38	0.02	0.36	0.12
F2-89-V94	1.70	1.68	0.560	0.534	0.150	0.137	0.030	0.039	4.82	0.83	0.02	0.81	0.17
F2-89-V95	1.72	1.80	0.600	0.567	0.160	0.160	0.030	0.039	5.91	0.93	0.03	0.90	0.24
F2-89-V96	1.71	1.80	0.730	0.701	0.170	0.160	0.040	0.046	4.48	0.48	0.01	0.46	0.11
F2-89-V97	1.79	1.80	0.600	0.567	0.140	0.137	0.030	0.040	4.14	0.66	0.02	0.64	0.15

[-x, analyzed by X-ray fluorecence; -icp, analyzed by ICP; LOI 925C, loss on ignition at 925 degrees C; n.a., not analyzed]

Appendix II. Concentrations of major elements in samples of sediment in cores from the continental slope in the Gulf of the Farallones.

Core	Latitude	Longitude	Depth-m	% SiO2-x	% Al2O3-x	% Al2O3-icp	% Fe2O3-x	% Fe2O3-icp	% MgO-x	% MgO-icp	% CaO-x	% CaO-icp	% Na2O-x	% Na2O-icp	% K2O-x
F8-90-G01	37.356	-123.248	1260	65.5	12.5	12.9	4.42	4.58	2.38	2.49	2.76	2.94	3.37	3.50	1.86
F8-90-G03	37.335	-123.198	1545	63.4	12.8	13.0	4.25	4.43	2.54	2.65	2.74	2.94	3.30	3.50	1.91
F8-90-G05	37.380	-123.178	960	63.8	12.7	12.9	4.76	4.86	2.50	2.49	2.67	2.80	3.56	3.77	1.90
F8-90-G07	37.400	-123.117	795	63.8	12.8	13.0	4.64	4.86	2.47	2.49	2.63	2.80	3.53	3.77	1.89
F8-90-G09	37.411	-123.079	716	66.2	12.5	12.9	4.89	5.15	2.54	2.49	3.04	3.22	3.19	3.37	1.78
F8-90-G10	37.428	-123.020	537	67.0	13.0	13.0	4.24	4.43	2.23	2.32	2.90	3.08	3.35	3.50	1.86
F8-90-G12	37.216	-123.409	3120	n.a.	n.a.	11.9	n.a.	5.58	n.a.	3.48	n.a.	1.82	n.a.	4.72	n.a.
F8-90-G17	37.343	-122.906	280	66.9	13.1	12.9	4.30	4.43	2.30	2.32	2.93	2.94	3.41	3.50	1.97
F8-90-G19	37.258	-123.051	670	66.5	12.6	12.7	4.40	4.58	2.17	2.16	2.74	2.94	3.37	3.50	1.86
F8-90-G21	37.224	-123.244	1605	n.a.	n.a.	13.0	n.a.	5.01	n.a.	2.65	n.a.	3.08	n.a.	3.64	n.a.
F8-90-G23	37.166	-123.015	630	65.8	12.5	12.7	5.09	5.29	2.31	2.32	2.88	3.08	3.24	3.37	1.87
F8-90-G24a	37.528	-123.408	2495	n.a.	n.a.	13.2	n.a.	5.72	n.a.	3.32	n.a.	2.10	n.a.	3.77	n.a.
F8-90-G24b	37.528	-123.408	2495	n.a.	n.a.	12.7	n.a.	5.43	n.a.	3.32	n.a.	2.38	n.a.	4.04	n.a.
F8-90-G25	37.450	-123.334	1720	57.3	12.2	12.7	5.23	5.29	2.97	2.98	2.59	2.66	3.78	4.18	1.93
F8-90-G27	37.433	-123.243	1378	65.0	13.0	13.2	4.39	4.58	2.51	2.49	2.86	2.94	3.05	3.24	1.87
F8-90-G28	37.455	-123.191	970	66.2	12.8	13.0	4.50	4.72	2.44	2.49	2.76	2.94	3.27	3.37	1.88
F8-90-G31	37.385	-123.080	728	65.0	12.9	13.0	4.54	4.72	2.43	2.49	2.72	2.80	3.40	3.50	1.90
F8-90-G32	37.314	-123.028	638	63.8	13.7	14.2	4.79	4.86	2.52	2.65	2.72	2.80	3.36	3.64	2.05
F8-90-G33	37.311	-123.154	1050	n.a.	n.a.	n.a.	n.a.	n.a.	n.a.	n.a.	n.a.	n.a.	n.a.	n.a.	n.a.
F8-90-G34	37.242	-123.074	685	67.3	12.7	12.9	4.60	4.72	2.21	2.16	2.67	2.80	3.14	3.24	1.90

[-x, analyzed by X-ray fluorescence; -icp, analyzed by ICP; LOI 925C, loss on ignition at 925 degrees C; n.a., not analyzed]

Appendix II. Concentrations of major elements in samples of sediment in cores from the continental slope in the Gulf of the Farallones.

Core	% K2O-icp	% TiO2-x	% TiO2-icp	% P2O5-x	% P2O5-icp	% MnO-x	% MnO-icp	% LOI 925C	% Total C	% Inorganic C	% Organic C	% CaCO3
F8-90-G01	1.80	0.57	0.58	0.14	0.14	0.040	0.048	5.57	1.28	0.07	1.21	0.58
F8-90-G03	1.92	0.60	0.60	0.16	0.16	0.040	0.045	7.56	1.61	0.15	1.46	1.23
F8-90-G05	1.92	0.58	0.58	0.16	0.16	0.040	0.045	6.64	1.23	0.08	1.15	0.69
F8-90-G07	1.92	0.58	0.58	0.17	0.18	0.040	0.046	6.72	1.32	0.08	1.23	0.70
F8-90-G09	1.80	0.65	0.63	0.15	0.16	0.050	0.058	4.15	0.61	0.03	0.58	0.24
F8-90-G10	1.80	0.55	0.53	0.14	0.14	0.040	0.048	4.22	0.67	0.04	0.63	0.30
F8-90-G12	1.92	n.a.	0.60	n.a.	0.18	n.a.	0.040	n.a.	3.42	0.10	3.33	0.79
F8-90-G17	1.92	0.52	0.52	0.14	0.14	0.040	0.046	4.05	0.59	0.03	0.55	0.28
F8-90-G19	1.80	0.56	0.55	0.14	0.14	0.040	0.046	4.84	0.90	0.07	0.83	0.55
F8-90-G21	1.92	n.a.	0.62	n.a.	0.16	n.a.	0.048	n.a.	1.89	0.15	1.74	1.27
F8-90-G23	1.80	0.60	0.62	0.14	0.14	0.040	0.053	4.89	0.85	0.03	0.82	0.25
F8-90-G24a	2.04	n.a.	0.67	n.a.	0.16	n.a.	0.044	n.a.	2.42	0.11	2.31	0.90
F8-90-G24b	1.92	n.a.	0.62	n.a.	0.18	n.a.	0.041	n.a.	3.19	0.16	3.03	1.33
F8-90-G25	2.04	0.61	0.60	0.19	0.18	0.040	0.043	12.70	2.59	0.02	2.57	0.17
F8-90-G27	1.80	0.62	0.60	0.15	0.16	0.040	0.049	5.89	1.32	0.13	1.19	1.10
F8-90-G28	1.80	0.59	0.60	0.15	0.14	0.040	0.049	4.75	0.88	0.05	0.83	0.40
F8-90-G31	1.92	0.58	0.57	0.15	0.16	0.040	0.048	5.72	1.03	0.08	0.95	0.64
F8-90-G32	2.04	0.63	0.63	0.15	0.16	0.040	0.053	5.37	0.66	0.03	0.62	0.27
F8-90-G33	n.a.	n.a.	n.a.	n.a.	n.a.	n.a.	n.a.	n.a.	1.05	0.13	0.92	1.05
F8-90-G34	1.80	0.55	0.53	0.14	0.14	0.040	0.046	4.22	0.66	0.02	0.65	0.13

[-x, analyzed by X-ray fluorescence; -icp, analyzed by ICP; LOI 925C, loss on ignition at 925 degrees C; n.a., not analyzed]

Appendix III. Concentrations of trace elements in samples of sediment in cores from the continental shelf in the Gulf of the Farallones.

Core	Latitude	Longitude	Depth (m)	ppm Ba	ppm Ce	ppm Co	ppm Cr	ppm Cu	ppm Ga	ppm La	ppm Li	ppm Nd	ppm Ni	ppm Pb	ppm Sc	ppm Sr	ppm Th	ppm V	ppm Y	ppm Zn
F2-89-V01	37.935	-123.389	119	870	32	8	150	6	11	18	24	16	35	6	8	250	6	63	11	48
F2-89-V02	37.956	-123.354	104	480	43	9	210	12	12	24	31	20	52	9	12	220	6	93	15	61
F2-89-V03	37.974	-123.320	108	550	53	9	150	20	8	29	25	24	37	10	10	470	10	79	10	56
F2-89-V04	37.995	-123.283	113	560	39	9	170	7	12	21	26	19	44	4	10	240	6	72	12	48
F2-89-V05	38.012	-123.247	110	560	52	8	330	11	13	29	27	23	43	9	11	250	6	80	14	61
F2-89-V06	38.027	-123.220	108	570	62	8	200	8	11	35	28	27	43	10	13	260	8	91	18	52
F2-89-V07	38.043	-123.184	99	490	31	9	130	16	12	17	36	17	60	12	12	230	7	89	13	63
F2-89-V08	38.062	-123.151	84	490	33	9	130	13	14	18	32	15	56	10	12	240	6	86	13	62
F2-89-V09	37.892	-123.357	113	550	52	10	170	8	12	29	28	22	46	9	11	260	7	85	15	51
F2-89-V10	37.913	-123.320	106	550	37	9	180	7	12	22	26	17	44	7	10	250	5	73	12	49
F2-89-V11	37.930	-123.285	106	520	73	10	260	7	11	39	26	30	46	10	14	270	7	100	20	52
F2-89-V12	37.947	-123.246	102	550	50	9	290	6	12	28	26	23	44	6	11	240	6	81	14	50
F2-89-V13	37.966	-123.210	102	550	85	10	280	8	12	46	27	34	44	7	14	270	8	100	21	51
F2-89-V14	37.980	-123.184	102	520	48	10	260	12	13	27	32	22	53	9	12	240	7	90	15	67
F2-89-V15	37.998	-123.152	90	490	31	9	130	14	12	17	33	14	58	6	12	230	4	87	13	63
F2-89-V16	38.018	-123.114	73	500	31	8	130	13	14	17	32	14	52	10	11	230	6	83	12	60
F2-89-V17	37.837	-123.323	117	550	38	9	140	9	12	21	28	18	47	10	11	270	5	80	13	51
F2-89-V18	37.858	-123.280	102	530	57	10	250	9	13	29	26	25	46	9	12	260	7	90	16	53
F2-89-V19	37.877	-123.244	99	560	43	8	220	8	14	23	27	19	44	4	11	240	5	75	13	50
F2-89-V20	37.896	-123.207	95	510	62	10	260	7	12	33	26	27	45	9	13	260	6	96	18	50
F2-89-V21	37.915	-123.172	95	490	98	11	310	9	14	54	27	41	47	9	16	270	9	120	24	54
F2-89-V22	37.929	-123.147	95	490	49	10	170	14	13	27	35	22	60	11	13	230	7	98	16	64
F2-89-V23	37.954	-123.105	82	480	33	9	130	14	13	18	33	16	58	9	12	230	6	85	13	62
F2-89-V24	37.956	-123.077	76	500	32	10	120	15	14	18	35	18	56	12	12	230	8	87	13	63
F2-89-V25	37.829	-123.115	86	650	28	6	100	6	10	16	10	13	26	5	6	250	4	48	9	31
F2-89-V26	37.845	-123.086	88	490	59	11	270	12	13	31	30	27	60	9	14	270	7	110	18	66
F2-89-V27	37.861	-123.058	88	540	38	9	150	9	12	21	27	17	49	7	10	230	6	75	13	49
F2-89-V28	37.878	-123.027	84	520	43	8	190	10	12	23	28	19	49	9	12	250	5	85	15	58
F2-89-V29	37.897	-122.995	73	530	35	8	150	11	14	19	27	16	46	7	11	250	5	76	13	55
F2-89-V30	37.914	-122.959	64	530	31	8	160	8	13	17	26	14	41	8	10	260	5	68	12	48
F2-89-V31	37.943	-122.907	46	530	36	7	160	7	11	22	23	17	35	7	9	220	5	68	12	48
F2-89-V32	37.969	-122.858	38	530	30	9	110	12	10	16	26	14	45	9	11	250	5	82	13	51
F2-89-V33	37.826	-122.974	74	580	31	7	170	8	11	18	25	15	37	5	8	240	5	61	10	46
F2-89-V34	37.844	-122.939	68	530	55	9	240	8	13	30	26	22	44	7	12	260	4	88	16	50
F2-89-V36	37.878	-122.882	59	500	30	9	140	12	14	17	26	16	47	10	11	270	5	79	12	56
F2-89-V37	37.892	-122.861	53	530	27	9	130	9	12	14	27	14	47	8	11	270	5	78	11	48
F2-89-V38	37.911	-122.832	40	520	29	10	130	9	15	15	25	15	47	12	11	260	7	82	12	48
F2-89-V40	37.743	-122.983	58	190	160	9	430	6	7	92	10	56	27	4	13	130	18	110	25	38
F2-89-V41	37.757	-122.958	58	560	27	7	100	5	10	16	21	14	33	6	7	240	5	61	10	33
F2-89-V42	37.776	-122.924	59	570	22	7	80	6	10	14	18	10	34	9	6	240	7	52	8	30
F2-89-V43	37.795	-122.888	55	470	130	20	460	10	10	69	24	49	60	10	20	290	10	170	28	72
F2-89-V44	37.814	-122.852	53	420	160	17	710	14	14	93	24	69	56	13	23	270	23	210	37	74

Appendix III. Concentrations of trace elements in samples of sediment in cores from the continental shelf in the Gulf of the Farallones.

Core	Latitude	Longitude	Depth (in)	ppm Ba	ppm Ce	ppm Co	ppm Cr	ppm Cu	ppm Ga	ppm La	ppm Li	ppm Nd	ppm Ni	ppm Pb	ppm Sc	ppm Sr	ppm Th	ppm V	ppm Y	ppm Zn
F2-89-V45	37.833	-122.819	48	540	25	9	130	10	11	15	25	14	44	5	9	240	6	67	10	43
F2-89-V46	37.856	-122.772	40	500	31	12	150	10	12	16	26	15	55	8	13	260	4	92	13	53
F2-89-V48	37.706	-122.903	57	570	29	8	150	6	10	17	20	13	38	11	7	260	4	64	10	34
F2-89-V50	37.742	-122.834	53	560	36	9	220	7	12	21	16	16	38	11	7	260	8	97	10	36
F2-89-V51	37.762	-122.804	53	430	150	20	580	20	10	77	22	57	56	10	20	270	34	210	29	73
F2-89-V52	37.786	-122.760	42	500	31	11	150	12	12	16	27	15	54	9	13	260	4	92	13	51
F2-89-V53	37.814	-122.713	31	500	30	12	140	11	13	16	26	14	57	9	12	250	5	92	12	53
F2-89-V54	37.620	-122.905	82	500	28	9	120	12	13	16	25	16	45	6	11	280	6	72	12	51
F2-89-V55	37.638	-122.872	69	490	33	9	150	10	12	18	26	16	44	8	12	280	5	81	13	50
F2-89-V56	37.651	-122.847	62	510	43	10	240	11	12	23	25	19	42	10	13	290	6	87	15	50
F2-89-V57	37.671	-122.815	53	460	96	14	1300	10	15	52	24	40	51	8	17	280	34	130	24	64
F2-89-V58	37.690	-122.782	51	470	75	12	340	11	12	40	24	32	46	12	17	290	12	120	21	54
F2-89-V59	37.708	-122.748	42	470	52	13	240	9	13	26	24	24	52	8	15	280	8	130	18	58
F2-89-V60	37.739	-122.694	33	480	33	12	180	10	13	19	25	17	57	9	13	260	7	100	13	53
F2-89-V61	37.761	-122.656	22	500	36	17	240	16	13	18	25	17	64	11	16	250	5	130	16	70
F2-89-V62	37.551	-122.898	99	500	42	12	190	11	13	22	25	20	54	9	15	310	7	99	16	57
F2-89-V63	37.572	-122.857	86	530	31	9	140	10	12	17	27	15	47	11	12	290	6	79	12	52
F2-89-V64	37.590	-122.825	73	510	33	10	150	10	14	17	25	15	46	9	12	290	5	81	13	51
F2-89-V65	37.603	-122.800	64	480	29	9	140	9	13	15	24	12	42	9	12	290	4	77	13	48
F2-89-V66	37.622	-122.765	53	500	33	9	150	9	13	17	23	16	41	5	12	290	5	81	13	46
F2-89-V67	37.641	-122.730	46	490	30	10	150	9	14	16	24	17	44	5	12	280	6	84	13	48
F2-89-V68	37.660	-122.696	38	510	26	10	120	9	11	14	26	11	46	10	12	270	<4	84	12	46
F2-89-V69	37.678	-122.666	33	490	31	13	170	9	12	16	25	15	56	7	14	270	5	100	13	53
F2-89-V70	37.691	-122.644	29	490	34	13	190	9	12	17	25	16	54	9	14	260	6	110	14	53
F2-89-V71	37.501	-122.840	91	460	49	15	240	11	13	26	24	23	58	9	18	310	9	130	19	63
F2-89-V72	37.520	-122.805	86	510	42	11	190	11	13	22	25	20	49	13	15	310	6	96	15	54
F2-89-V73	37.539	-122.772	73	500	30	9	120	10	14	16	24	13	44	8	12	300	4	78	12	49
F2-89-V74	37.553	-122.749	66	490	29	10	140	10	14	16	24	15	43	7	12	300	5	78	12	49
F2-89-V75	37.573	-122.715	55	510	29	9	120	8	13	15	25	13	43	7	12	290	<4	78	12	45
F2-89-V76	37.592	-122.681	66	510	31	9	140	9	14	17	25	14	46	6	11	290	4	80	12	46
F2-89-V77	37.612	-122.648	38	520	29	10	130	9	12	15	25	15	49	8	12	280	5	85	12	49
F2-89-V78	37.639	-122.602	29	500	39	13	210	10	13	21	23	20	52	7	14	280	5	110	16	54
F2-89-V79	37.658	-122.564	25	510	35	12	150	9	13	18	23	17	50	5	13	270	4	96	14	51
F2-89-V80	37.429	-122.768	88	540	47	14	230	11	15	24	23	22	53	9	17	320	5	120	17	59
F2-89-V81	37.452	-122.733	81	520	34	10	140	10	13	18	23	17	43	13	13	310	4	84	13	47
F2-89-V82	37.470	-122.701	73	520	30	9	120	10	13	15	25	15	43	9	12	300	5	78	12	48
F2-89-V83	37.480	-122.679	68	500	29	9	120	10	13	16	24	15	42	9	12	300	4	75	12	49
F2-89-V84	37.500	-122.642	59	530	29	8	120	9	13	15	24	15	39	12	11	300	4	73	12	44
F2-89-V85	37.521	-122.610	51	530	37	9	160	9	14	20	24	16	42	6	12	320	4	83	14	49
F2-89-V86	37.547	-122.565	35	600	34	9	120	7	12	19	21	17	38	6	11	370	6	79	14	45
F2-89-V87	37.421	-122.650	82	520	33	9	130	10	14	17	24	15	41	7	12	310	6	75	12	50
F2-89-V88	37.429	-122.626	69	530	42	9	160	8	15	23	23	20	42	8	12	310	7	79	14	49

Appendix III. Concentrations of trace elements in samples of sediment in cores from the continental shelf in the Gulf of the Farallones.

Core	Latitude	Longitude	Depth (m)	ppm Ba	ppm Ce	ppm Co	ppm Cr	ppm Cu	ppm Ga	ppm La	ppm Li	ppm Nd	ppm Ni	ppm Pb	ppm Sc	ppm Sr	ppm Th	ppm V	ppm Y	ppm Zn
F2-89-V89	37.446	-122.582	58	520	65	13	230	9	14	34	21	30	45	12	15	330	11	110	19	54
F2-89-V90	37.462	-122.548	45	540	42	11	260	8	15	27	19	26	37	8	13	350	8	93	17	47
F2-89-V91	37.855	-123.177	95	520	48	8	170	7	11	26	26	20	41	9	12	250	4	83	15	47
F2-89-V92	37.875	-123.142	93	490	83	10	330	9	13	46	27	36	49	8	16	260	9	120	23	56
F2-89-V94	37.905	-123.085	88	500	35	9	160	12	13	20	30	16	53	8	11	220	5	79	13	62
F2-89-V95	37.921	-123.055	77	500	32	9	130	13	13	17	32	16	54	8	12	240	4	83	13	58
F2-89-V96	37.935	-123.032	66	530	42	9	220	11	14	23	28	23	45	10	12	250	8	81	16	54
F2-89-V97	37.952	-123.000	58	520	33	9	220	11	14	19	29	17	45	7	10	240	6	77	13	55

Appendix IV. Concentrations of trace elements in samples of sediment in cores from the continental slope in the Gulf of the Farallones.

Core	Latitude	Longitude	Depth (m)	ppm Ba	ppm Ce	ppm Co	ppm Cr	ppm Cu	ppm Ga	ppm La	ppm Li	ppm Nd	ppm Ni	ppm Pb	ppm Sc	ppm Sr	ppm Th	ppm V	ppm Y	ppm Zn
F8-90-G01	37.36	-123.25	1260	570	40	12	140	18	14	21	31	20	66	7	13	280	6	93	14	71
F8-90-G03	37.33	-123.20	1545	610	38	11	150	25	14	20	37	19	73	4	12	270	7	98	15	79
F8-90-G05	37.38	-123.18	960	560	39	11	140	26	12	21	33	18	67	7	12	280	6	95	14	74
F8-90-G07	37.40	-123.12	795	560	39	11	140	20	13	20	33	18	69	6	12	280	6	95	14	72
F8-90-G09	37.41	-123.08	716	520	46	12	160	16	11	24	26	21	63	5	13	300	8	95	16	64
F8-90-G10	37.43	-123.02	537	540	36	12	140	16	11	19	26	14	57	5	12	310	<4	84	13	60
F8-90-G12	37.22	-123.41	3120	1000	36	10	150	87	10	20	51	20	100	6	10	180	6	110	10	140
F8-90-G17	37.34	-122.91	280	540	33	11	110	12	12	18	27	16	53	8	11	320	5	79	12	57
F8-90-G19	37.26	-123.05	670	540	38	10	140	14	11	21	25	17	54	3	11	300	5	86	13	61
F8-90-G21	37.22	-123.24	1605	650	42	12	160	27	13	22	36	19	77	8	13	280	7	100	15	86
F8-90-G23	37.17	-123.01	630	530	42	11	160	19	12	22	24	20	55	8	12	300	7	93	14	73
F8-90-G24a	37.53	-123.41	2495	800	42	13	150	59	15	21	57	19	100	8	15	200	9	120	15	120
F8-90-G24b	37.53	-123.41	2495	830	37	13	150	64	14	21	50	18	100	6	14	210	8	110	14	120
F8-90-G25	37.45	-123.33	1720	700	39	12	140	42	14	21	45	19	85	10	14	240	7	100	14	100
F8-90-G27	37.43	-123.24	1378	580	41	12	140	23	13	21	34	18	72	3	13	280	6	97	15	73
F8-90-G28	37.45	-123.19	970	550	43	12	140	17	16	21	29	23	67	11	12	290	9	94	14	69
F8-90-G31	37.39	-123.08	728	540	37	11	140	19	12	20	32	17	65	7	12	290	6	92	14	69
F8-90-G32	37.31	-123.03	638	580	43	13	130	29	15	23	43	20	67	12	13	290	8	100	15	75
F8-90-G33	37.31	-123.15	1050	490	40	20	170	75	8	23	29	20	89	6	9	370	6	110	20	110
F8-90-G34	37.24	-123.07	685	550	39	10	150	19	13	21	25	18	56	4	11	300	5	85	13	73